KERNFORSCHUNGSZENTRUM

KARLSRUHE

Mai 1974 KFK 1968

Institut für Angewandte Systemtechnik und Reaktorphysik
Projekt Schneller Brüter

Method to investigate neutron inelastic cross section data by analyzing fast nanosecond decaying spectra

N. Pieroni

GESELLSCHAFT
FÜR
KERNFORSCHUNG M.B.H.

KARLSRUHE

Als Manuskript vervielfältigt

Für diesen Bericht behalten wir uns alle Rechte vor

GESELLSCHAFT FÜR KERNFORSCHUNG M.B.H.
KARLSRUHE

KERNFORSCHUNGSZENTRUM KARLSRUHE

1974 KFK 1968

Institut für Angewandte Systemtechnik und Reaktorphysik
Projekt Schneller Brüter

Method to investigate neutron inelastic cross section data by analyzing fast nanosecond decaying spectra

by

N. Pieroni[+)]

[+)] Comisión Nacional de Energía Atómica, Argentina

A thesis submitted in partial fulfillment of the requirements for the degree of DOCTOR EN FISICA, UNIVERSIDAD DE CUYO, ARGENTINA

Gesellschaft für Kernforschung mbH., Karlsruhe

Method to investigate neutron inelastic cross section data by analyzing fast nanosecond decaying spectra

Abstract

A method to test and improve neutron inelastic scattering cross section data of reactor materials was developed. It is based on the large sensitivity of fast nanosecond decay leakage spectra of small pulsed systems to the inelastic scattering process. By analyzing the decaying spectra in small energy intervals, quantitative changes in the inelastic cross section data can be introduced to provide agreement between calculation and measurement. In this manner adjusted data can be defined.

The method required the use of a reliable spectrometric procedure to measure fast nanosecond time-dependent spectra and an appropriate time-dependent spectra computational procedure. A NE 213 liquid scintillator detector was used in the measurements. The Karlsruhe Monte-Carlo program KAMCCO was adapted for the calculations performed in this study.

The method was applied to the study of an iron and a natural uranium system. It was possible to define adjusted inelastic cross section data for iron and ^{238}U. The reliability of the information obtained by the present method was verified through independent experiments.

14.5.1974

Eine Methode zur Untersuchung der Daten von inelastischen Streuquerschnitten durch die Analyse von schnellen Neutronenspektren, die in Nanosekunden zerfallen

Zusammenfassung

Zur Überprüfung und Verbesserung der Daten von inelastischen Neutronenstreuquerschnitten für Reaktormaterialien wurde eine neue Methode entwickelt. Sie beruht auf der starken Abhängigkeit des Zerfalls eines Feldes schneller Neutronen in einer kleinen gepulsten Anordnung von den inelastischen Streuprozessen. Der Zerfall des Neutronenausflußspektrums wird nach Injektion eines Neutronenpulses im Nanosekundenbereich mit guter Energieauflösung analysiert. Durch Änderungen der inelastischen Streuquerschnittsdaten wird eine Übereinstimmung von Rechnung und Messung herbeigeführt und ein Satz angepaßter Daten gewonnen. Die Methode erfordert deshalb eine zuverlässige Technik zur Messung von zeitabhängigen Neutronenspektren im Nanosekundenbereich und ebenso eine adäquate Rechenmethode. Als Detektor wurde ein NE 213 Flüssigkeitsscintillator verwendet. Zur Berechnung der zeitabhängigen Spektren wurde eine modifizierte Version des Karlsruher Monte-Carlo-Programms KAMCCO angewandt.

Die Methode wurde bei der Untersuchung von Eisen- und Natururansystemen angewendet. Für Eisen und Natururan wurden angepaßte inelastische Streuquerschnittsdaten erhalten. Die Zuverlässigkeit, der auf diese Weise gewonnenen Daten, wurde durch andere unabhängige Experimente bestätigt.

ACKNOWLEDGEMENTS

The present work was done during a two year fellowship granted by the International Atomic Energy Agency under the auspice of the Comisión Nacional de Energía Atómica, Argentina. This time was spent in the Kernforschungszentrum Karlsruhe, at the Institut für Angewandte Systemtechnik und Reaktorphysik, under the direction of Professor Dr. W. Häfele, who I would like to thank for providing me a place to work. I would also like to thank Dr. F. Helm, head of the SNEAK-Physik Department, for his kind support, as well as the support provided through the Internationales Büro of the Kernforschungszentrum Karlsruhe by Dr. H. Laue. I also thank DP. M. Küchle for allowing me to perform the experiment in the fast subcritical facility SUAK and for his critical review of the work.

I am especially indebted to my advisor, Dr. E. Wattecamps, who suggested the subject of the present work and who continuosly provided guidance during its realization. Dr. D. Rusch provided invaluable assistance that I would especially like to recognize. I would also like to thank Dr. H. Borgwaldt for his constant assistance. I am grateful to Dr. P. Mc Grath for his valuable help.

The generous assistance received from members of the staff of the Institut für Angewandte Systemtechnik und Reaktorphysik, and of the Institut für Neutronenphysik und Reaktortechnik, during the performance of this work is acknowledged.

Finally I would like to mention the friendly atmosphere provided by the people at the Kernforschungszentrum Karlsruhe. This contributed not only to my work, but also made my stay pleasant.

CONTENTS

List of Tables

List of Figures

Chapter I

OVERVIEW

Inelastic scattering is the dominating process in the energy degradation of fast neutrons by heavy elements. Therefore, in fast reactors, which typically contain large amounts of heavy materials, inelastic scattering provides the main contribution to the slowing down of fast fission neutrons.

The inelastic scattering cross section data, $\sigma(n,n')$, of many reactor materials, due to their present discrepancies, limit the accuracy of reactor calculations. Therefore a more precise determination of $\sigma(n,n')$ is of high priority, primarily for uranium, plutonium and iron, which are by far the most important inelastic scatters in nuclear reactors. As an example, for ^{238}U changes in its inelastic scattering cross section, $\sigma^{28}(n,n')$, smaller than its present estimated discrepancies /1,2/, produce variations in the calculated effective multiplication factor k_{eff} of fast critical facilities and power reactors as large as, or greater than, the variation produced by a 5 % change in the fission spectrum /3/. A 15 % decrease in $\sigma^{28}(n,n')$ can change the k_{eff} of a fast reactor as much as 2.7 % /3/.

The temporal behaviour of the neutron population in a pulsed system can provide valuable information on neutron interactions and, in particular on the inelastic scattering interactions. The main process responsible for the energy degradation during the early decay of the neutron spectra is the inelastic scattering. An accurate interpretation of the measurements is possible if the assembly studied consists of a single element arranged in a simple geometry.

Time-dependent reaction rate measurements were performed by Gozani /4/ in a subcritical spherical depleted uranium system. In this experiment a solid state detector with a ^{235}U or ^{237}Np foil neutron converter was used. Therefore implied in the measurement is the energy integration according to the energy dependence of the fission cross section of ^{235}U or ^{237}Np. Nevertheless, this experiment demonstrated the possibility of using a

measurement of this type to test the inelastic scattering cross section data of ^{238}U in the energy region above several hundred KeV.

In the work presented here an improvement of the previous experiment is obtained by measuring time-dependent spectra in small energy intervals. In this case the sensitivity of these spectra to the inelastic scattering cross section data is increased appreciably with respect to the sensitivity of the time-dependent reaction rates of ^{235}U or ^{237}Np /5/.
In addition, the capability of the present method is not limited to the testing of the inelastic scattering cross section data. The practical advantage of this method is that it permits one to introduce quantitative changes of inelastic scattering data in an appropriate calculational procedure to provide agreement between calculation and measurements. In this manner adequate corrections to the data are possible.
This is, therefore, an independent method, which shares the simplicity and cleaness of decay measurements of small pulsed assemblies, to obtain information on the inelastic scattering cross section data of materials of interest in fast reactors.

The development of this method required, 1) a reliable spectrometric procedure to measure fast nanosecond time-dependent spectra, and 2) a time-dependent spectra computational procedure appropriate for adjusting the inelastic cross section data.

To measure time-dependent fast neutron spectra, a NE 213 liquid scintillator was used since it allows both fast timing and neutron spectrometry by pulse height analysis in a large dynamic range. The detector was placed at the surface of the pulsed assembly and the detector events were recorded in a time and pulse height analyzer. The pulse height spectrum in each time channel was unfolded to obtain the neutron spectrum. A computer program (TRADI) was developed to deduce the neutron spectra from measured pulse height distributions. In the TRADI procedure, the pulse height distribution is transformed into a proton energy distribution by the use of the measured relation between pulse height and proton energy. Under the assumption of a constant energy distribution of the recoil protons, the neutron spectrum can be obtained by differentiation of the proton recoil distribution. The use of the measured transformation function between the

proton energy and the resulting pulse height avoided relying on a transformation measured by others with similar but not identical detectors. In addition, intrinsic characteristics of the detector used could be taken into account.

The reliability of the detector and the associate program TRADI was verified by measuring known spectra. These included monoenergetic neutron sources, the spontaneous fission neutron spectrum of a californium source, and the continuous spectra from pulsed sources. This investigation demonstrated that the NE 213 liquid scintillator, combined with the unfolding TRADI procedure, is adequate for the measurement of time-dependent fast neutron spectra of pulsed small assemblies in the energy range from 0.4 MeV to 6 MeV, or higher if the flux is small above 6 MeV. Within this energy range the systematic error is ± 10 %.

The spectrometer was applied to the measurement of the time-dependent leakage spectra of two small assemblies built in the fast subcritical facility SUAK /6/. One was made of natural iron and the other of natural uranium. The assemblies were cylinders of about 30 cm diameter and 20 cm height. The NE 213 liquid scintillator and the pulsed neutron source were located on the axial axis at the surface of opposite faces. Neutron bursts of 2 nsec width at 5×10^4 pps frequency from a D(T,n)α generator provided the approximately 14 MeV monoenergetic neutron source /7/.

Two experimental runs were performed for each assembly,

- a low amplification run covering the energy range from 1.2 MeV to 8 MeV analyzed in 512 pulse height channels and eight time channels of 4.1 nsec each;
- a high amplification run covering the energy range from 0.4 MeV to 2.2 MeV analyzed in 512 pulse height channels and eight time channels of 8.2 nsec each.

Each resultant two-dimensional distribution consisted of eight pulse height spectra. The TRADI program was applied to obtain the neutron spectra. These spectra were integrated to obtain group fluxes with lethargy intervals of about 0.3 .

The two-dimensional measurements were also analyzed by integrating to provide the time-integrated pulse height spectrum. This pulse height spectrum was processed by TRADI to provide the time-integrated, or stationary, spectrum.

In the interpretation of these measurements the Monte-Carlo program KAMCCO /8/ was used to obtain the time-dependent leakage spectra. The input cross section data were based upon the KEDAK nuclear data file /9/. The KAMCCO program uses an analytical fit to the differential cross section data points. The spectra were calculated in energy groups and time intervals equal to the ones used in the measurements.
Stationary spectra were also obtained with the KAMCCO program. Typical statistical errors in the calculated group fluxes were about 10 % for the time-dependent spectra and about 5 % for the stationary spectra. This accuracy was obtained with a calculation time of about 10 min for the iron and about 30 min for the uranium assembly on the IBM 370/165 computer.
The KAMCCO program was adapted so that changes in the nuclear input data could be introduced. Therefore it was possible to make a parametric investigation of the influence of variations in the $\sigma(n,n')$, $\sigma(n,2n)$ and $\sigma(n,f)$ data. It was found that inelastic scattering is the dominating mechanism that determines the shape of the fast decaying spectra, and that these spectra are very sensitive to slight changes in the inelastic scattering cross section data. Quantitative changes in the inelastic scattering cross section data could therefore be introduced to achieve better agreement between the measured and the calculated spectra. In this manner it was possible to define adjusted inelastic scattering cross section data for iron and ^{238}U.

The reliability of the adjusted data obtained by the present method was verified through independent experiments.
The adjusted data for iron was used in the calculation of the leakage spectrum of a small iron assembly with a californium source.
The adjusted data for ^{238}U was used in the calculation of a fast reactor core which was particularly sensitive to ^{238}U data.
In both cases the improvement in the agreement with the experimental results demonstrated the reliability of the information obtained by the present method.

Chapter II

EXPERIMENTAL PROCEDURE

II.1 Description and operation of the NE 213 scintillator

In the measurement of time-dependent fast neutron spectra one must typically perform fast timing and pulse height measurements in a dynamic range of 400:1. In the entire dynamic range the fast trigger must not have an appreciable pulse height dependence, or "walk".

A NE 213 liquid scintillator of 5.08 cm diameter and 5.08 cm height was coupled to a RCA 8050 photomultiplier (PM) with an ORTEC 270 base having a "constant fraction of pulse height" trigger (CFPHT). A simplified block diagram of the NE 213 detector electronics is shown in Fig. 1, in which one can recognize the three primary components: the time-of-flight (TOF) analysis, the rise time analysis for the neutron-gamma discrimination, and the pulse height analysis. The construction and adjustment of this detection system was performed by Rusch /10,11/. The Section II.1 is included here only for the sake of completeness.

II.1.1 The neutron-gamma discrimination

The neutron-gamma discrimination system utilized the cross-over technique /12/, with expanded dynamic range, by the use of two amplifiers (No. 1 and No. 2) and two timing single channel analyzers (SCA). The SCA's trigger at the trailing edge on a constant fraction of the pulse height. The trigger fraction F was modified to a nominal value of 0.8, which corresponds to 20 % of the peak pulse height. This particular neutron-gamma discrimination system was selected for the following reasons:

a) The discrimination properties are slightly better than those obtained with the combination of double-delay line shaped signals and a zero cross over detector. The latter is equivalent to F = 0.5
b) The difference in the rise time measurement between neutron and gamma scintillation increases with increasing F-value. That means that a large F-value reduces the requirements on the stability of the circuit. However the selection of large F-values is limited by the circuit's higher sensitivity to noise.

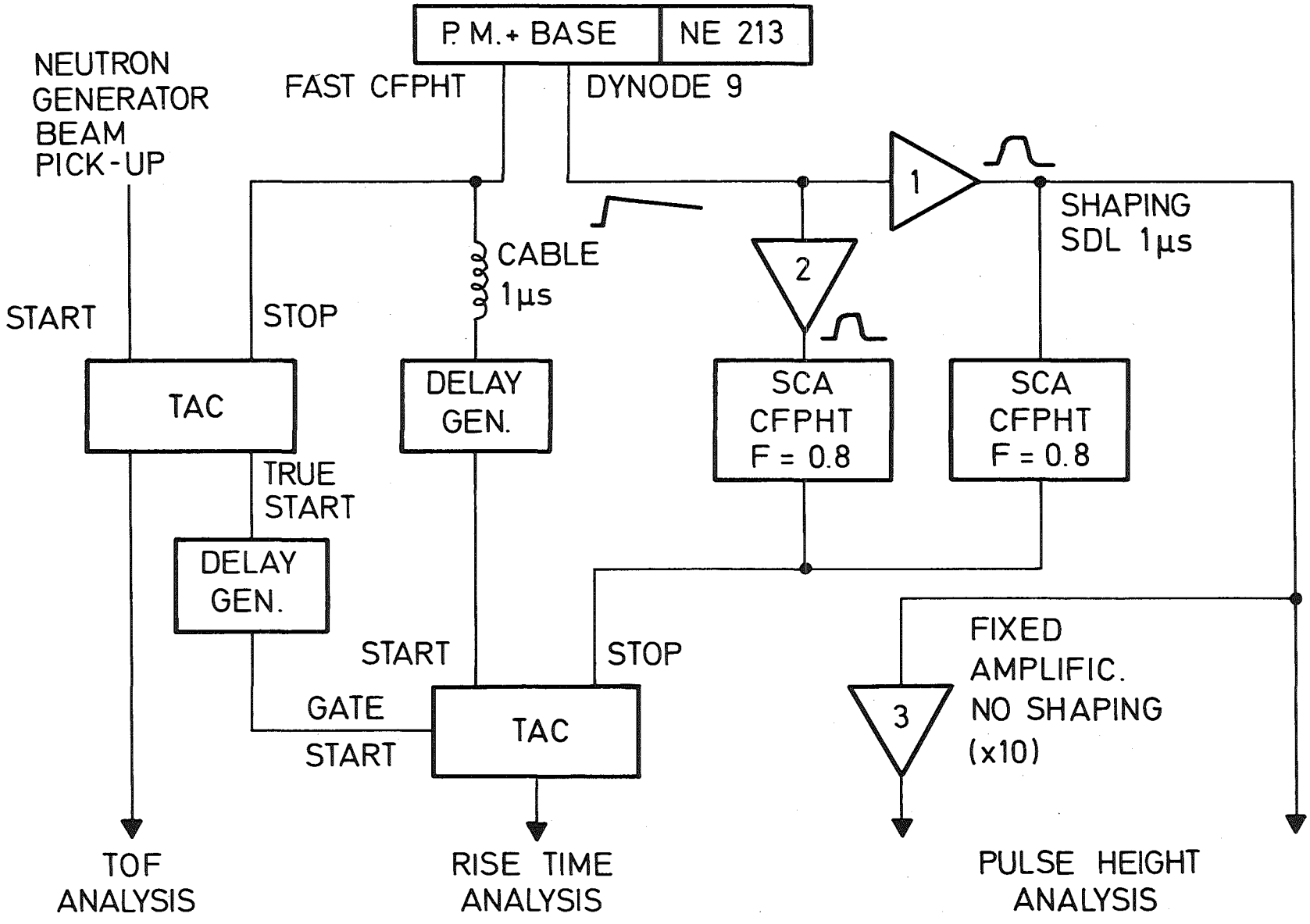

Fig.1 Simplified block-diagram of the NE 213 detector electronics

Amplifier No. 2 in the discrimination circuit, Fig. 1, was set to about twenty times the amplification of No. 1. Since it is only possible for one event to exist at a given time, in the cross-over detection system the range of the signal levels of both branches can be adjusted.
For the measurements on assemblies with high gamma-ray background, the start of the rise time measurements in the time-to-amplitude-converter (TAC) was gated synchronously with the accelerator to reduce dead time losses.

II.1.2 Timing adjustments

Because of the scintillation properties of the NE 213 scintillator one obtains different current signals for neutrons and gammas. Therefore the timing adjustment was done with monoenergetic neutrons from a time-of-flight experiment. The "walk" was investigated with the detector at a distance of 3 meters from a bare target of 14 MeV pulsed neutron source with a 2 nsec burst width /7/. Virtually no "walk" was found in the pulse height range from 1 to 100 times the threshold. In the range from 100 to 200 a "walk" of 1 nsec was observed. For higher pulses the heavy overload of the ORTEC 270 discrimination system caused an erroneous triggering which occurred 8 nsec earlier than it did under normal operation. The dynamic range of the fast discriminator could have been expanded by a signal splitting procedure similar to the logic used in the neutron-gamma discrimination system. However, this was not necessary for the experiments intended, because the timing becomes uncertain only at energies greater than 9 MeV.

II.1.3 Pulse height analysis

The pulse height distributions were measured with two different amplifications in consecutive runs. A first amplification (amplifier No. 1) was adjusted to record the upper edge of the 14 MeV response near the upper end of the analyzer scale, and the second run was performed with ten times higher amplification (amplifiers No. 1 plus No. 3) covering the lower end

of the pulse height scale.
The measured response to 14 MeV neutrons is shown in Fig. 2. No correction for alinearity and losses in the neutron-gamma discrimination was applied. The function is compared with the result of Verbinski et al. /13/ from whom the pulse height scale was taken. The pulse height unit of our measurement was chosen to give close agreement in the structure of both distributions. The structures of the response functions agree well up to one light unit. The differences at the upper end are attributed to alinearity in our photomultiplier. The pulse height spectra of a ^{22}Na source, used for gain calibration, is also shown in Fig. 2 , The pulse height unit, as defined in Ref. /13/, is 1.13 times the half-height of the Compton edge of the 1.28 MeV gamma-ray of ^{22}Na. However we found that for our detector this factor should be 1.21 . To clear this discrepancy approximately 100 response functions were measured by a simultaneous analysis of the time-of-flight and pulse height distribution from a fast decaying tailored source /14/. By adjusting the time channel width in the time-of-flight measurement, monoenergetic neutrons with an energy resolution of 4 % at 1 MeV could be obtained. The pulse height distributions corresponding to each time channel were the response functions of these monoenergetic neutrons. The half-height of the upper edge of each response function, as a function of the neutron energy -which corresponds to the maximum recoil proton energy-, together with the values of Verbinski et al. /13/ and Smith et al. /15/ are shown in Fig. 3 . Up to 2 MeV our values agree with those from Ref. /13/. Our detector is very similar to the one used by Verbinski et al. /13/, but the gamma- an proton-light yield relationships are different.

II.2 The data evaluation program TRADI

In the determination of a neutron spectrum one often encounters the problem of unfolding a measured proton recoil pulse height distribution. To obtain the neutron spectrum from pulse height distributions several methods have been developed. Generally these methods entail the use of rather complex time-consuming computer programs. However, for experiments with the NE 213 liquid scintillators, in which most of the neutron flux is in the energy range between 0.4 MeV and 6 MeV, one is able to use a simple and flexible procedure. This procedure, which is used in the program TRADI developed for this study, relies on the transformation of the pulse

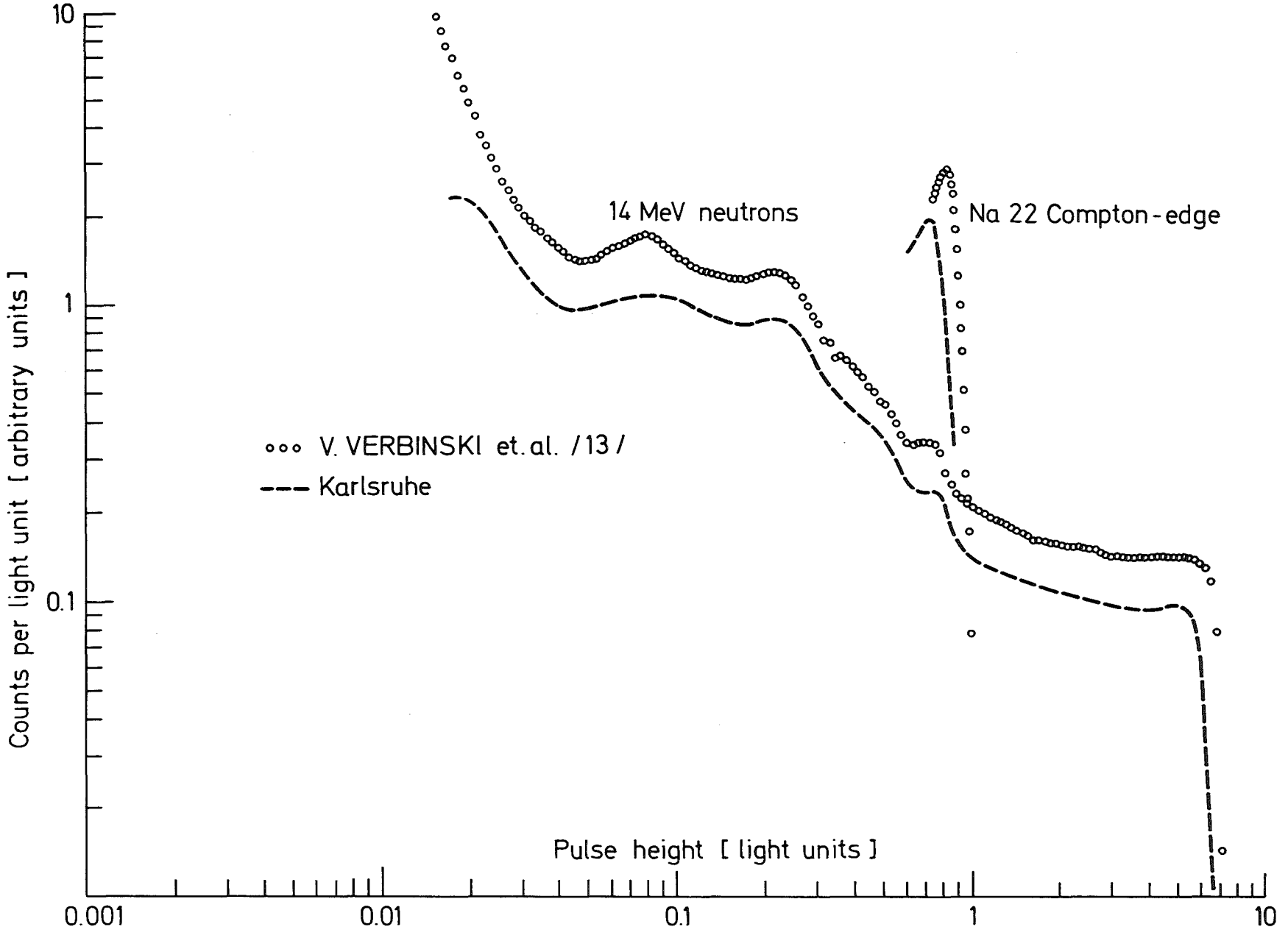

Fig. 2 Comparison of measured response functions. The light unit is defined in text, Section II.1.3

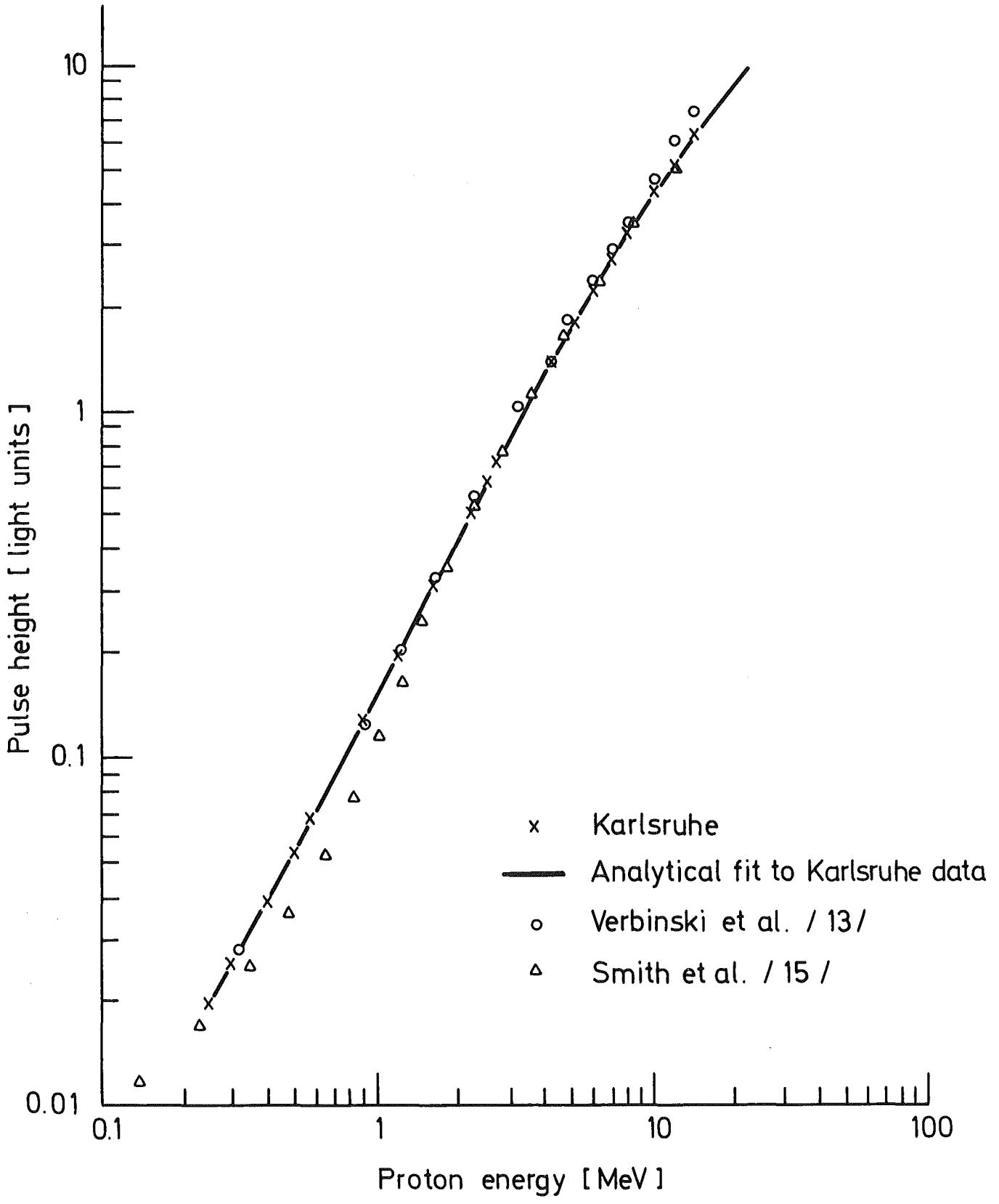

Fig.3 Pulse height - proton energy relation of the NE-213 scintillator

height to recoil proton energy. This transformation is based upon the measured function of pulse height to proton energy of the particular detector used. A constant energy distribution of the recoil protons is assumed, thus allowing one to obtain the incident neutron spectrum by a differentiation of the measured pulse height distribution. This results in a very simple code which can be easily modified to the requirements of the experiment being unfolded.
The mathematical expressions used in the program are presented in the following. In the Appendices an input description of the program with a sample problem are provided, in addition to a Fortran source listing.

II.2.1 Transformation of pulse height to proton energy

A proton of energy E_p will produce a given quantity of scintillation light determined by the intrinsic characteristics of the recoil proton detector. This, in turn, through a linear amplification by the associated electronic system, yields a pulse height (V). The measured transformation function between the proton energy and the resulting pulse height is approximated by a polynomial of the form

$$\log\left(\frac{E_p}{E_o}\right) = \sum_{i=1}^{6} A_i \left[\log\left(\frac{V}{V_o}\right)\right]^{i-1} \qquad (1)$$

where E_o and V_o are calibration constants.
The least squares program LESQU /16/ is applied to fit the measured response of the detector to monoenergetic neutrons to obtain the coefficients A_i. The resultant fit for the NE 213 detector used in our experiments is shown in Fig. 3 . The coefficients A_i are given in Table I.
With this procedure one does not have to rely on a transformation function measured by others for similar detectors, but which do not necessarily have identical characteristics. This can be appreciated in Fig. 3 where the results of measurements of Verbisnki et al. /13/ and Smith et al. /15/ for the NE 213 scintillator are also shown.

Therefore this procedure allows one to take into account the intrinsic characteristics of the detectors, for example, in our case the alinearity at higher energies.

Table I

Coefficients of the proton energy-pulse height transformation function

Normalization: $\frac{V}{V_o}$ = 1.51 E+04 for 14 MeV neutrons

i	A_i
1	-1.57761955
2	0.32292497
3	0.26951498
4	-0.07669628
5	0.00476279
6	0.00064185

II.2.2 Derivation of the neutron flux from the proton distribution

The proton energy distribution $P(E_p)$ is given by /17,18/

$$P(E_p) = \int_{E_p}^{En} N_H \cdot V_d \cdot \Phi(E_n) \cdot \sigma_H(E_n) \cdot K(E_n, F_p) \cdot dE_n \qquad (2)$$

where

E_n incident neutron energy

N_H hydrogen atoms/cm^3

V_d detector volume

$\sigma_H(E_n)$ (n,p) cross section

$K(E_n,E_p)$ recoil proton spectrum

$$\Phi(E_n) = \Phi_o(E_n) \cdot f(\omega L, E_n) \tag{3}$$

where

$\Phi_o(E_n)$ incident neutron flux per unit energy

$f(\omega L, E_n)$ attenuation factor given by

$$f(\omega L, E_n) = \frac{1 - e^{-\omega L}}{\omega L} \tag{4}$$

where

L detector lenght

$$\omega = N_H \cdot \sigma_H(E_n) + N_C \cdot \sigma_C(E_n) \tag{5}$$

N_C graphite atoms/cm^3

$\sigma_C(E_n)$ total neutron cross section of graphite

Assuming a constant recoil proton spectrum

$$K(E_n,E_p) = \frac{1}{E_n} \quad , \tag{6}$$

differentiation of Eq. (2) yields

$$\Phi_o(E_n) = - \frac{E_n}{N_H \cdot V_d \cdot f(\omega L, E_n) \cdot \sigma_H(E_n)} \cdot \frac{d}{dE_p} P(E_p) \tag{7}$$

II.2.3 Efficiency, double scattering and wall effect corrections

The counter efficiency is defined by the expression /19,20/

$$\varepsilon(E_n,L) = N_H \cdot \sigma_H(E_n) \cdot L \cdot f(\omega L,E_n) \qquad (8)$$

The double scattering and wall effect corrections are introduced by /19,20/

$$\eta(E_n,R,L) = 1 - C_1 \cdot R_{max}(E_n) + C_2 \cdot \sigma_H(E_n) + C_3 \cdot \sigma_H(0.068\ E_n) \qquad (9)$$

where

$$C_1 = 0.78/L \qquad (10)$$

$$C_2 = 0.090\ L \cdot N_H \cdot 10^{-24} \qquad (11)$$

$$C_3 = 0.077\ R \cdot N_H \cdot 10^{-24} \qquad (12)$$

R detector radius

$$R_{max} = 1.18 \times 10^{-3}\ E_n^{1.75} \qquad (13)$$

The analytical values for the cross sections for hydrogen and graphite are determined from the following equations /17/

$$\sigma_H(E_n) = 3\Pi \left(1.206\ E_n + (-1.86 + 0.09415\ E_n + 0.0001306\ E_n^2)^2\right)^{-1} + \Pi \left(1.206\ E_n + (0.4223 + 0.13\ E_n)^2\right)^{-1} \qquad (14)$$

$$\sigma_C(E_n) = 2.285\ E_n^{-0.425} \qquad (15)$$

The final expression for Eq. (7) is

$$\Phi_o(E_n) = - \frac{E_n}{\pi R^2 \cdot \varepsilon(E_n,L) \cdot \eta(E_n,L,R)} \cdot \frac{d}{dE_p} P(E_p) \qquad (16)$$

II.3 Verification of the spectrometric procedure

To test the reliability of the detector and the associated unfolding procedure, pulse height distributions obtained from monoenergetic neutrons with an energy resolution of 4 % at 1 MeV, and from continuous spectra were evaluated.

II.3.1 Monoenergetic spectra

The results of the TRADI evaluation of four monoenergetic neutron sources are shown in Fig. 4. The fluctuations below these spectrum peaks come from scintillation pile-up caused by multiple scattering in the detector. Scintillation pile-up increases with decreasing neutron energy because of the increasing cross section of the hydrogen in the detector. The differentiation of the resulting response functions results in a peak at the correct neutron energy. However below the peak energy the derivative changes sign giving a negative flux. If the height of the upper edge of the response function is taken as representing the height of an ideal rectangular distribution, the neutron flux is overestimated. In the case of a continuous spectrum this overestimation is compensated at a given energy by the negative flux evaluated for neutrons with slightly higher energies. This compensation for the continuous spectra is provided in the evaluation method by the corrections for double scattering and wall effects.

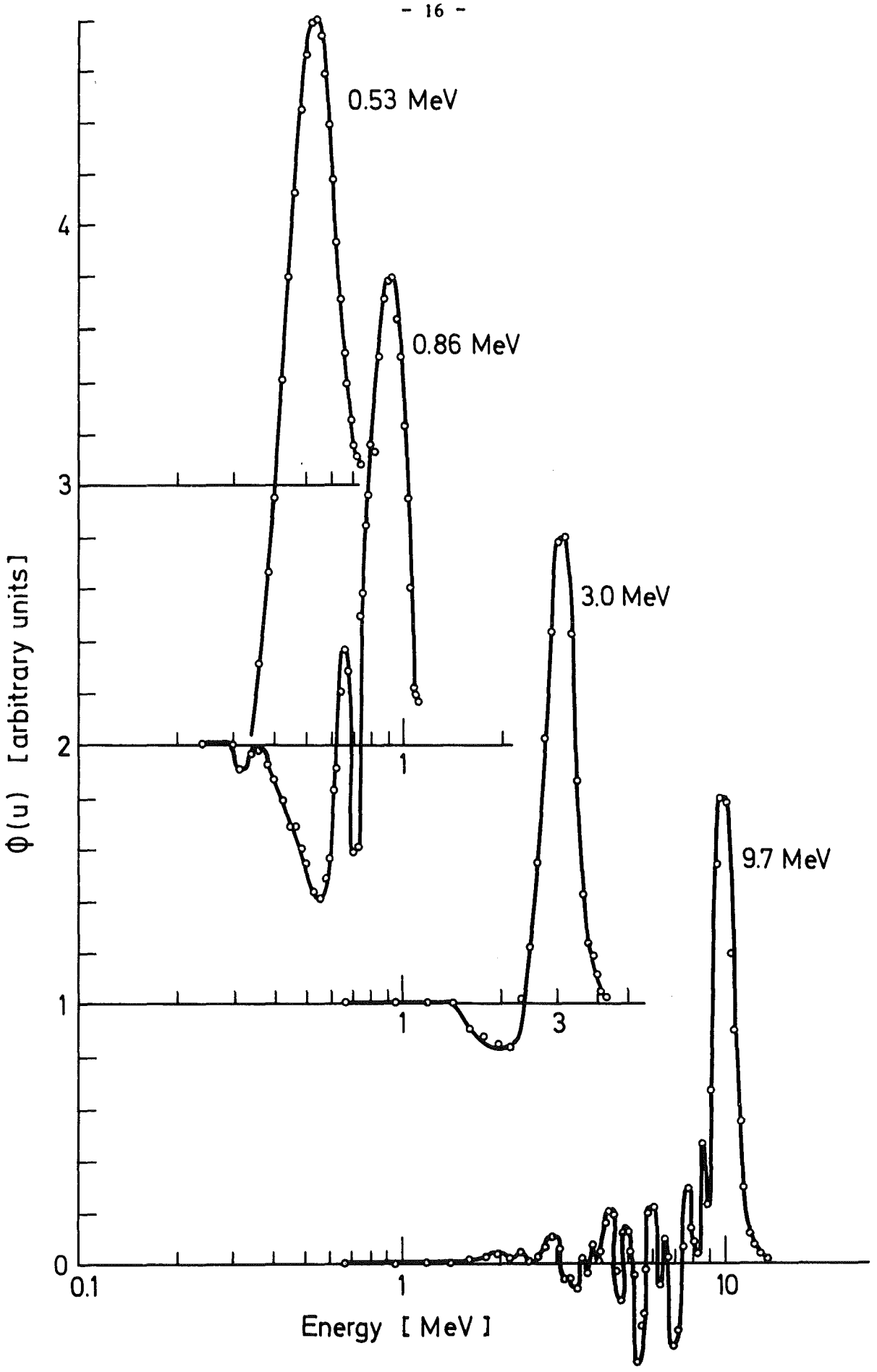

Fig.4 "TRADI" procedure applied to measured response functions

II.3.2 Continuous spectrum from a californium source

An additional test of the spectrometer was performed by measuring the spontaneous fission neutron spectrum of a ^{252}Cf source. The measurement can be performed with negligible statistical errors and several measurements with reliable techniques are available for comparison.
The pulse height distribution from our measurement was unfolded with the TRADI program as explained above. In addition, having proved that our detector is almost identical to the one of Ref. /13/, primarily in the low energy range, one may also use the FERDOR unfolding program /21/ with its included response matrix from Ref. /13/ for the NE 213 scintillator. The results from these two unfolding procedures are shown in Fig. 5 along with spectrum measurements performed by Werle and Bluhm /22/. A Maxwellian distribution fitted to the experimental spectra yields the Maxwellian energies given in Table II.
The TRADI results are consistent with those of Werle and Bluhm. As both TRADI and FERDOR evaluations utilized the same pulse height distributions the deviations in the results must be systematic. The shift in the spectrum between the two procedures is not due to a calibration error. Rather it results from two different sources. First, due to the assumed shape of the response function in TRADI the lower energy portion of the spectrum is underestimated. The FERDOR results do not contain this error. In the higher energy range the lower FERDOR results are due to the difference between the response functions in FERDOR and that of our detector (Fig. 3). In principle the FERDOR procedure is more accurate for the general unfolding problem, but it requires the response matrix of the particular detector used. In addition to perform the unfolding each pulse height spectrum must be measured in the entire range of the response matrix. The additional difficult experimental work required for the use of FERDOR is not worthwhile in view of the accuracy obtained with TRADI for spectra with small flux above 6 MeV. **For neutron energies above 6 MeV, the effect of the (n,α) reactions in the detector can invalidate the approximation of constant response function assumed in the TRADI procedure.**

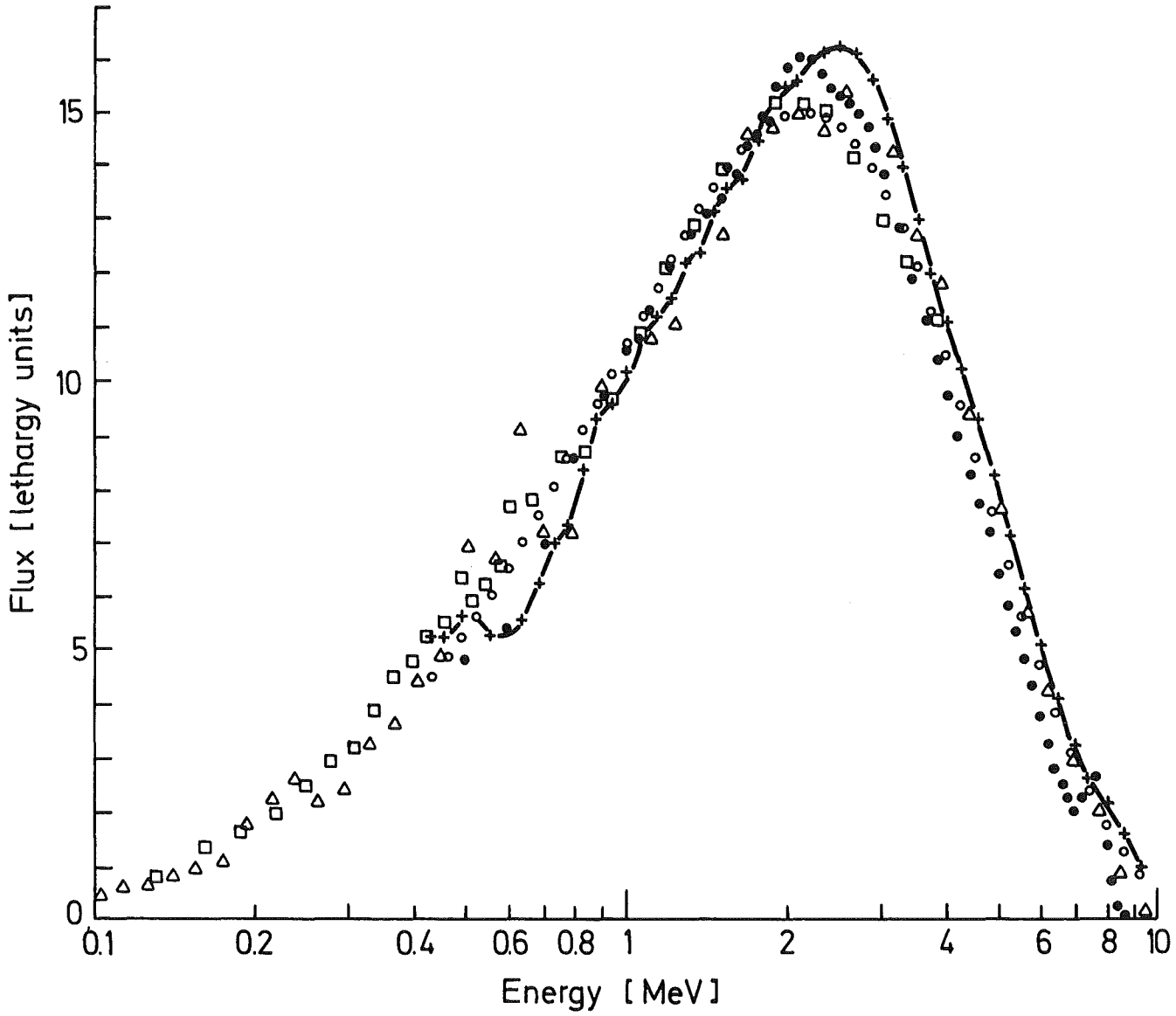

+ NE - 213 measurement, present investigation, TRADI unfolding

• NE - 213 measurement, present investigation, FERDOR unfolding

△ Proton recoil measurement, Bluhm and Werle [22]

□ ^{3}He measurement, Bluhm and Werle [22]

○ Maxwellian distribution, Maxwell - Energy = 2.135 MeV

Fig. 5 Spontaneous fission neutron spectrum of a Californium source
(fluxes normalized from 0.5 to 4.0 MeV)

Table II

Comparison of Maxwellian energies for the fission spectrum of ^{252}Cf

Reference	Fitting interval MeV	Maxwellian energy MeV
Present investigation, TRADI unfolding	1.0 - 7.0	2.135
Present investigation FERDOR unfolding	1.0 - 7.0	1.972
Werle and Bluhm /22/, proton recoil measurement	1.5 - 7.0	2.155
Werle and Bluhm /22/, ^{3}He measurement	1.0 - 4.0	2.130
Barnard et al. /23/, combined average	-	2.13
Knitter et al. /24/, TOF-measurement	0.15 - 15.0	2.13

II.3.3 Continuous spectra from pulsed sources

The detector can be used in the time-of-flight mode and in the pulse height analysis mode /25/. A two-dimensional measurement of pulse height and time-of-flight is particularly suited for a detailed test of the evaluation procedure. Integrating the spectra over the time-of-flight variable provides a pulse height spectrum which can be evaluated. Integrating the spectra of the same measurement over the pulse height variable provides a time-of-flight distribution. The errors in the time-of-flight mode are small and known /14/. Starting from the known time-of-flight spectrum any desired spectrum can be produced by an appropriate choice of the integration parameters. In Fig. 6 the results of both techniques are compared. In the upper energy range, where pulse height spectra from 2.4 MeV to 6 MeV neutron energy were integrated, the TRADI evaluation reproduces this portion of the spectrum correctly. For the lower energy part, the pulse height spectra corresponding to neutron energies from 1.1 MeV to 0.4 MeV were integrated, thus excluding neutrons of higher energies. Although the multiple scattering in the detector becomes dominant, the error compensation is still present.

II.4 The pulsed iron and uranium assemblies

The spectrometer was applied to measure the time dependent leakage spectra of two small assemblies built in the fast subcritical facility SUAK /6/.

The iron assembly, ZYLFE 3020, was constructed of cylindrical layers of natural iron to form a cylinder 15.0 cm radius and 20.3 cm height.

The uranium assembly, ZYLU 3020, was constructed of natural uranium blocks of 5.08 cm x 5.08 cm x 2.54 cm to form an approximate cylinder of 15.70 cm equivalent radius and 20.32 cm height.

The assemblies were supported in two small horizontal rails. They in turn were supported by four steel legs on an iron plate of 4.0 cm thickness at a distance of approximately 36 cm from the assembly.

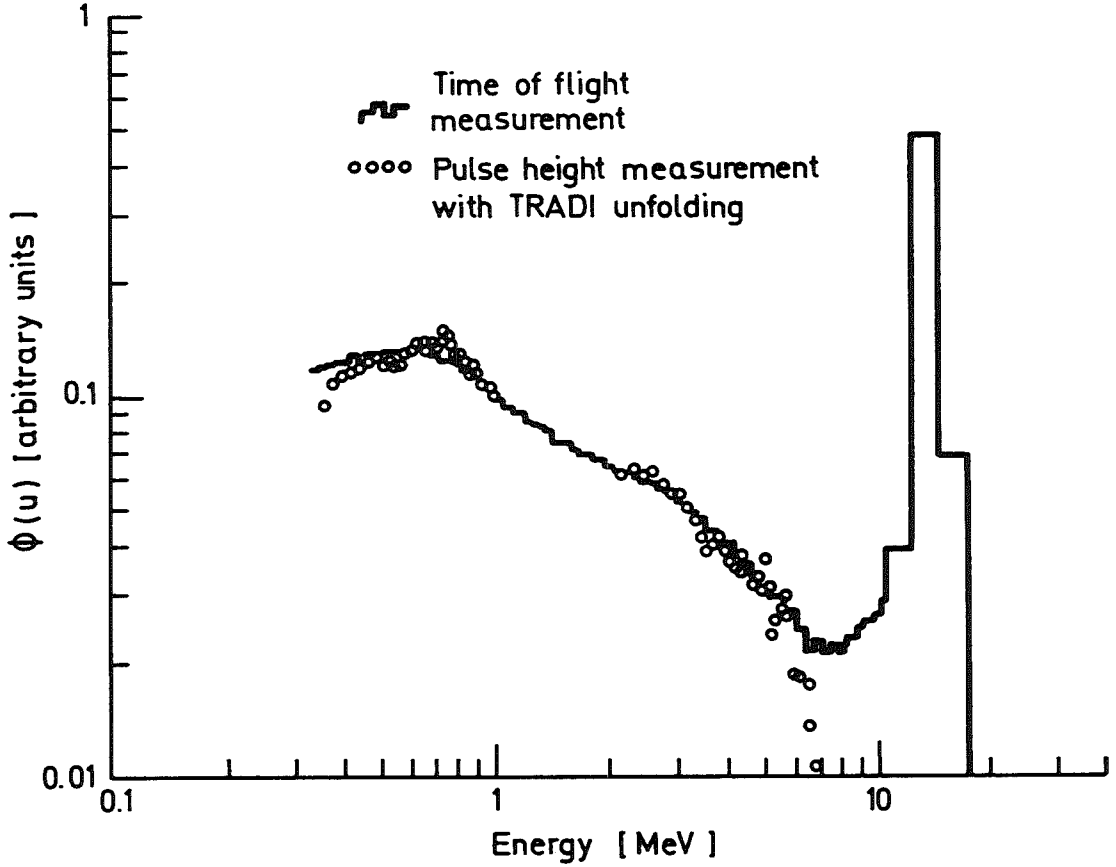

Fig.6 Comparison of "time-of-flight" and "pulse-height TRADI" spectra

The NE 213 liquid scintillator was placed at one of the flat faces along the cylinder axis. For the case of the ZYLU 3020 assembly, a lead layer of 0.9 cm thickness was placed between the assembly and the detector to shield the high gamma-ray activity (induced in the uranium blocks in previous experiments).
The target of the accelerator drift tube of the pulsed neutron generator was placed at the opposite flat face along the cylinder axis. A 160 kV accelerator with a high frequency deuteron ion source and a tritiated target was used /26/. The target yielded isotropically monoenergetic 14 MeV neutrons by the D(T,n)α reaction. A technique to provide a pulsed neutron source of 2 nsec burst width at 5 x 10^4 pps was used /7/. The burst width was 2 nsec at FWHM, 5 nsec at FW.1M, and 11 nsec at FW.01M. The neutron yield was 2 x 10^4 neutrons per burst. The pulse shape at the target and the neutron yield were continuously monitored by observing the associated α-particle with a NE 810 plastic scintillator.
The idealized experimental systems are shown in Figs. 7 and 8.

II.5 Measurement of the time-dependent spectra

In each assembly the pulse height analysis was performed with 512 pulse height channels and eight time intervals of 4.1 nsec each in the low amplification run (energy range from 1.2 MeV to 14 MeV) and respectively eight time intervals of 8.2 nsec each in the high amplification run (energy range from 0.4 MeV to 2.2 MeV).
The pulse height amplifications were verified to be identical to the ones used in the measurement of the pulse height to proton energy relation (Section II.2.1). This was done by reproducing the location of the ^{22}Na gamma-ray Compton edge and the edge of the 14 MeV neutron response function.
Dead time count losses were negligible since the intensity of the source was reduced so that the average counting rate for all signals was below 0.1 per burst. Thus the probability of obtaining two or more events within a burst was less than 0.5 %.

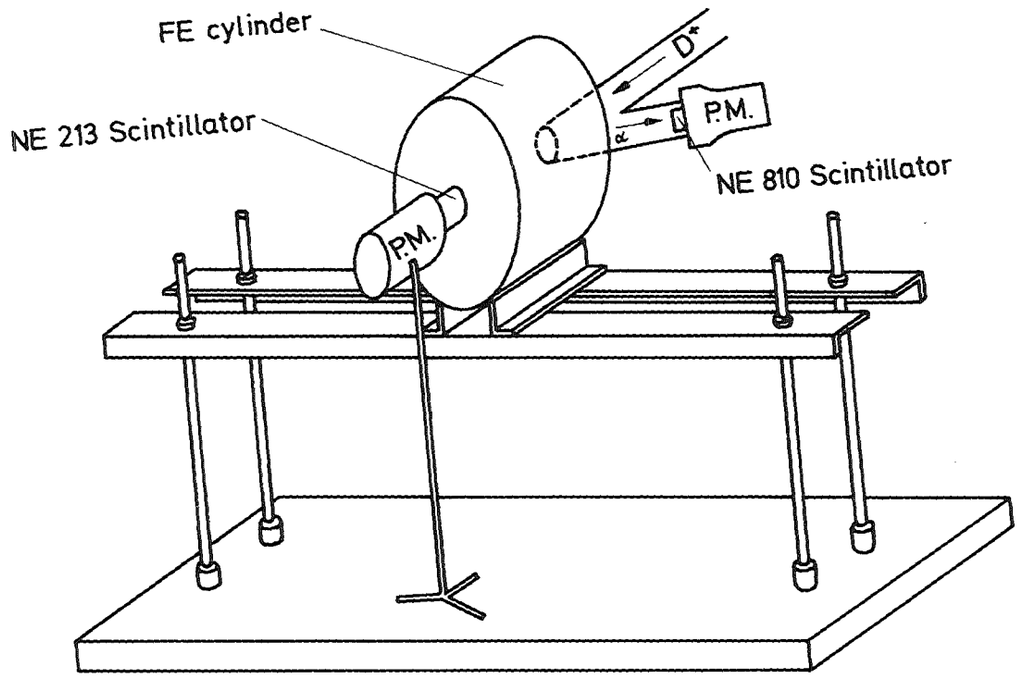

FE cylinder

radius	15.0 cm
height	20.3 cm
composition	99.99 % natural iron

Fig.7 Idealized Experimental Iron Assembly ZYLFE 3020

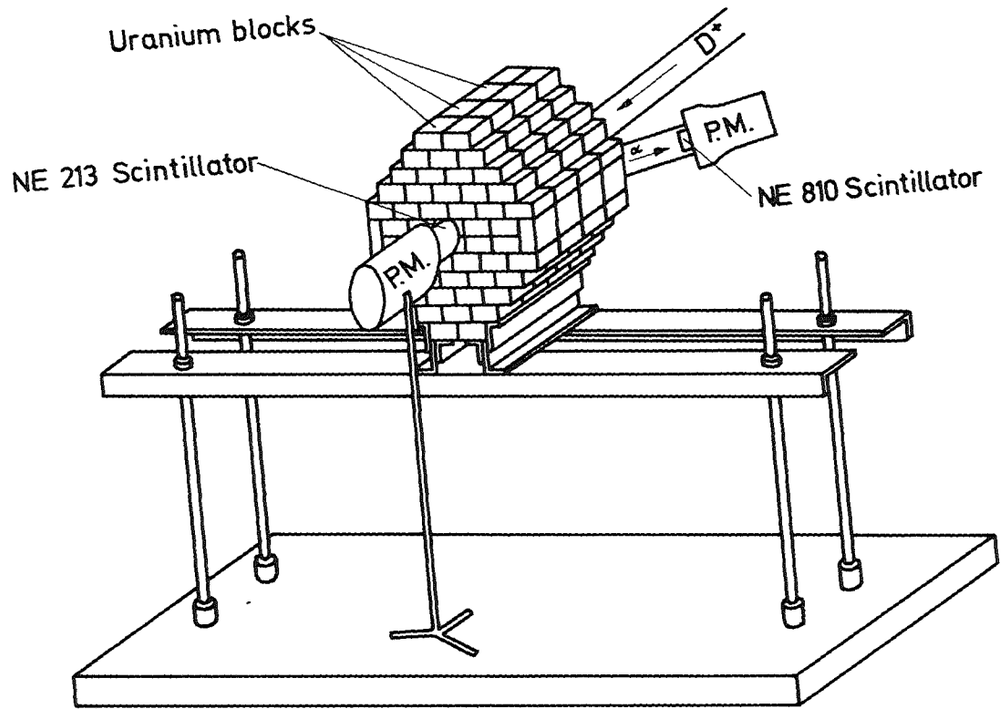

Uranium block

dimensions	5.08 cm x 5.08 cm x 2.54 cm	
composition	(10^{22} atoms / cm^3)	
	^{238}U	4.741 E+00
	^{235}U	3.440 E-02
	Ni	1.571 E-02

Fig. 8 Idealized Experimental Uranium Assembly ZYLU 3020

To eliminate the large contributions of direct 14 MeV neutrons a previously measured 14 MeV neutron response function was subtracted before evaluation of the pulse height spectra by the TRADI unfolding. From time-of-flight measurements it was known that the assembly had a small flux in the energy region (8 MeV to 12 MeV) where the pulse height distribution is almost entirely produced by the 14 MeV neutrons. Therefore the 14 MeV response function in the energy region from 8 MeV to 14 MeV was normalized to the measured pulse height spectrum. The selection of a different normalization region affects the results negligeably.

The neutron spectra were integrated to obtain group fluxes with lethargy intervals of about 0.3 . The count rate in the broad energy groups was large enough that statistical errors were negligible compared to systematic errors, which are estimated to be less than or equal to 10 %.

The two-dimensional measurements were also analyzed by integrating to provide the time integrated pulse height spectrum, yielding the stationary spectra.

Chapter III

INTERPRETATION PROCEDURE

III.1 The Monte-Carlo program KAMCCO

In the interpretation of the measured results the Karlsruhe Monte-Carlo program KAMCCO /8,27/ was used. This particular program was selected for the following reasons:

a) The KAMCCO program provides a means of calculating time-dependent fast neutron spectra of pulsed assemblies.

b) Relative changes in the input nuclear data can be introduced.

The KAMCCO option used in this study followed a census schema, i.e., neutrons with predetermined source coordinates are started at a prefixed time. These neutrons, and also all progenies, are followed up to a given time limit.

Three dimensional systems, with divisions into regions, can be calculated describing exactly the experimental assembly studied.

Nuclear data sets for KAMCCO were prepared from the KEDAK data file /9/ by the code DASU /28/ and the associated code DACONT /29/. During the random walk, cross sections are computed on a per isotope basis from data in core storage. For each isotope and cross section type a specific energy grid is used to perform a linear interpolation in the non-resonance regions. Inelastic scattering is described at discrete levels or, at high energy, through the evaporation model. Elastic scattering retains first order anisotropy in the center-of-mass system and involves transformation to the laboratory system.

Of importance for the present study is that the KAMCCO output provides the neutron spectra analyzed in variable energy- and time-intervals, which can be adjusted to the ones used in the measurements.

The KAMCCO program was changed by introducing new subroutines adapted for the requirements of the present experiment. The calculation flow diagram of the programs is shown in Fig. 9.

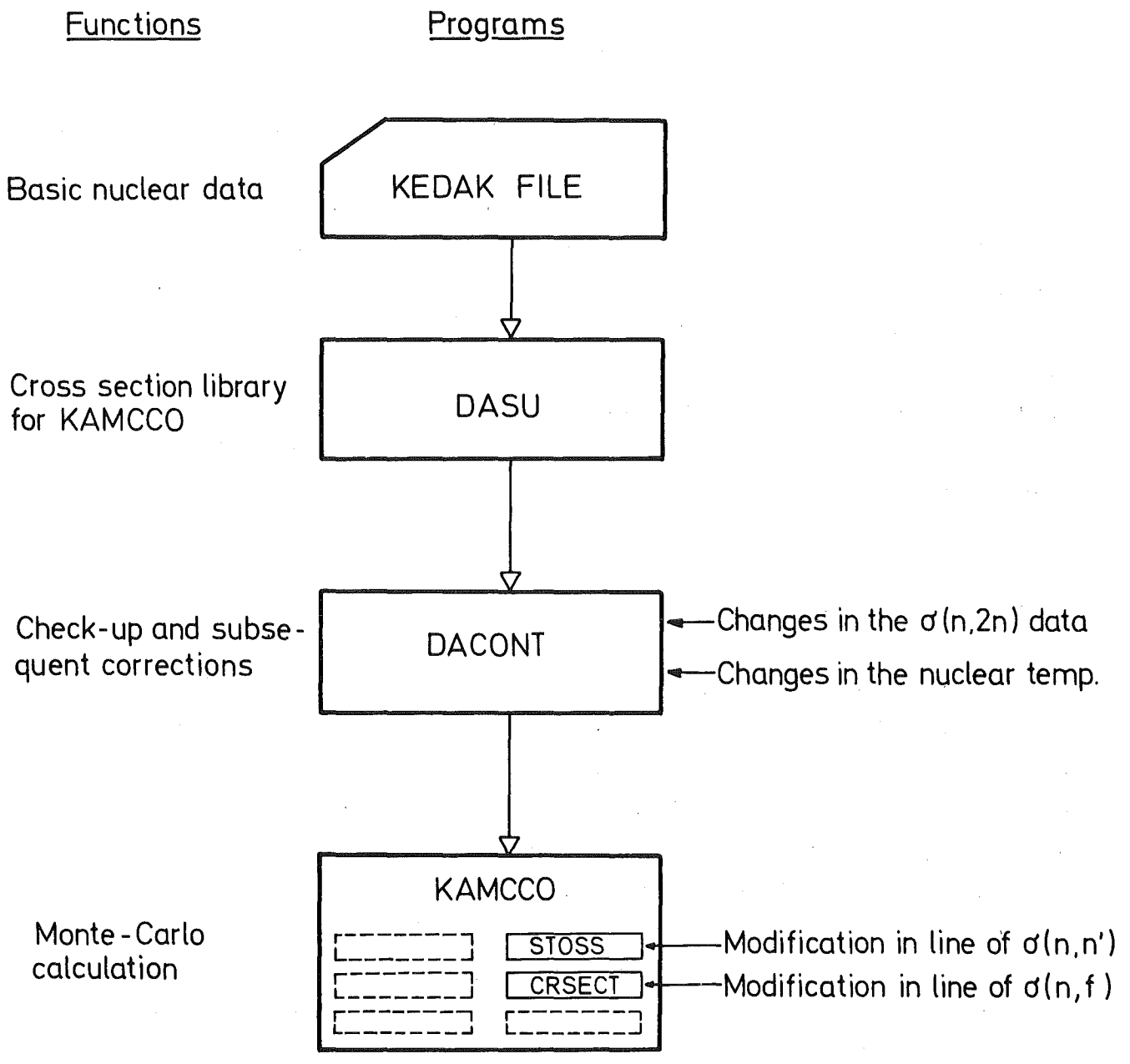

Fig. 9 Calculational Flow Diagram

The STOSS subroutine /30/ selects the type of collision process taking place in the random walk on the basis of the microscopic cross section data. Access was provided to modify in-line the original inelastic scattering cross section data. This is the main feature of the KAMCCO program suited to create adjusted data for the inelastic scattering process.
The CRSECT subroutine /30/ provided access to modify in-line the fission cross section data of ^{238}U. It allowed one to investigate the sensitivity of this data in the calculations for the present study.
The sensitivity of the calculations to the (n,2n) data and to the nuclear temperature in the evaporation model could be investigated by introducing changes in the corresponding data through the input provided by the associate program DACONT.

III.2 Most sensitive parameters in this experiment

The fast leakage spectrum of a small assembly, after injection of a 14 MeV neutron burst, is primarily determined by fission (for the case of the uranium assembly), (n,2n) and inelastic scattering processes. The sensitivity of the calculated leakage spectra, to the corresponding data, was investigated using the KAMCCO and associated programs. Typical changes in the time dependent leakage spectra of the uranium and iron assemblies, due to changes in the nuclear data, are presented in Table III. The estimation of the percent changes in the decaying spectra were obtained by observing the overall behaviour of each energy group. The energy groups in Table III correspond to the valid energy span covered in the present experiment.

III.2.1 Sensitivity to fission data

The accuracy of the KEDAK data for ^{235}U fission cross section is estimated to be 10 % /31/. To estimate the sensitivity of the calculation to the ^{238}U fission data, a extreme case was simulated, in which the fission

Table III

Sensitivity of calculated leakage spectra to nuclear data

Group	Energy MeV	Absolute percent changes in the leakage spectra							Calculation Accuracy %
		ZYLU 3020 Assembly				ZYLFF 3020 Assembly			
		σ(n,f) + 20 %	σ(n,2n) - 100 %	Nucl T + 30 %	σ(n,n') - 20 %	σ(n,2n) - 100 %	Nucl T + 20 %	σ(n,n') + 20 %	
5	5.11 - 6.50	3	12	10	36	3	1	45	10
9	1.87 - 2.50	2	9	0	34	1	1	35	5
13	0.56 - 0.80	2	3	0	20	1	1	30	3

cross section was increased by 20 %. The results in Table III show that, even in this extreme case, the influence is negligible compared to the statistical accuracy of the calculation.

III.2.2 Sensitivity to (n,2n) data

The (n,2n) cross section for ^{238}U and for Fe was drastically decreased by 100 % (i.e., this cross section was set equal zero). The numbers in Table III show that for the uranium assembly the leakage spectra changes a litle greater than the statistical accuracy of the calculation. It was therefore assumed that the inaccuracies of the (n,2n) cross section data for ^{238}U, estimated to be < 10 % /31/, have a negligible influence on the decaying leakage spectra.
For the iron assembly the changes were found to be negligible.

III.2.3 Sensitivity to the nuclear temperature

As the inelastic scattering at high energy is calculated with the evaporation model, the sensitivity to the nuclear temperature parameter was also tested. For ^{238}U, where the evaporation model is applied above 2 MeV, the nuclear temperature was increased by 30 %. As seen in Table III, only the highest energy group shows an effect comparable to the calcultional accuracy. Inaccuracies of the magnitude tested here are not expected in the nuclear temperature. Therefore the sensitivity to the inaccuracies of this parameter is estimated to be negligible for the ^{238}U study.
For Fe the evaporation model is applied above 5 MeV. A 20 % increase in the nuclear temperature implied negligible changes in the leakage spectra, as shown in Table III.

III.2.4 Sensitivity to the inelastic scattering data

The large sensitivity of fast decaying spectra to changes in the inelastic scattering cross section had been previously demonstrated for the case of ^{238}U /5,32/. To provide a quantitative comparison with the competing effects studied, Table III gives the changes resulting from a 20 % decrease in $\sigma(n,n')$ for ^{238}U and a 20 % increase in $\sigma(n,n')$ for Fe. These results reflect the fact that the inelastic scattering process is by far the most important effect in fast decaying spectra, and that these spectra are very sensitive to slight changes in the $\sigma(n,n')$ data.
It is important to remark that in the present work only the total inelastic cross section was modified, while the inelastic scattering matrix remained unaltered.

III.3 Time-of-flight distortion

To avoid excessively long calculations to obtain a convenient statistical accuracy, the time-dependent leakage spectra were calculated through the face were the detector was placed rather than include the detector in the calculation. However, in the measurement the detector can detect neutrons that have originated from all points on this face. Therefore the detected neutrons have variable flight paths from their origin at the surface of the system to the detector. Accordingly there is a time-of-flight distortion in the observed time behaviour. To estimate this distortion a KAMCCO calculation was performed for a geometry exactly representing the ZYLFE 3020 system with the detector. This calculation took appreciable longer than the calculation of the leakage through the face. The calculated spectra at the detector in this case showed a shifting of about 1 nsec. This shifting is of the order of the timing accuracy of the measurements.

III.4 Influence of back-scattered neutrons

To study the possible influence of back-scattered neutrons from the iron plate that supported the assemblies, two KAMCCO calculations for a spherical natural uranium system of approximately the same volume as the ZYLU 3020 assembly were performed. In one case the uranium sphere was bare,

in the other case it was covered with an iron spherical cell 4.0 cm thick at a distance of 36 cm from the uranium sphere. The neutron spectrum for the uranium sphere was the same in both cases, thus proving that there were no back-scattered neutrons perturbating the measurement. This theoretical result was verified by two time-of-flight measurements, in which the measured system was an iron cylinder, 30.0 cm diameter and 15.0 cm lenght, with and without a 5.0 cm thick iron plate placed at 25.0 cm from the iron cylinder. Above 600 KeV the measured spectra were identical within at least 2 %.

III.5 Calculation of the time-dependent spectra

The decaying leakage spectra of the ZYLFE 3020 and ZYLU 3020 assemblies were calculated with the KAMCCO program in energy groups of lethargy about 0.3 . The time behaviour was calculated in a sequence of 4.1 nsec and 8.2 nsec. Thus, the calculation had the same time-energy structure of the measurements.

Typical statistical errors in the calculated group fluxes are about 10 %, or less, for the time-dependent spectra and about 5 % for the stationary spectra. To obtain this accuracy, about 75 000 neutron histories were followed for the ZYLFE 3020 calculation, which required a computation time of about 10 minutes on the IBM 370/165 computer. For the ZYLU 3020 calculation, about 90 000 histories were needed, requiring a computation time of about 30 minutes.

Relative changes in the inelastic scattering cross section data were introduced in the KAMCCO program. By a trial-and-error procedure, ADJUSTED cross section data for ^{238}U and for iron could be found to provide agreement between calculated and measured results.

Chapter IV

RESULTS

The measured and calculated results of time- and energy-dependent, and stationary fluxes, are presented in Figs. 10 to 12 for the ZYLFE 3020 assembly, and in Figs. 14 to 16 for the ZYLU 3020 assembly. The experimental values are normalized to equal arbitrary source intensity, while the calculated values are normalized to one source neutron. To compare experiments and calculations a normalization factor was determined by adjusting graphically measured and calculated results to provide the minimum relative deviation in the time dependent group fluxes corresponding to the central energy range of this study. As it is seen in Figs. 12 and 16, this implied a normalization in the flux integrals in the energy range between 1 and 4 MeV.

IV.1 Results of the iron assembly.

As it was expected, the most sensitive test is the comparison of time-dependent spectra, as seen in Figs. 10 to 12. The calculation based upon the KEDAK data disagrees appreciably from the measured time behaviour for energies below 3 MeV. When the ADJUSTED set for the inelastic scattering cross section, as found by the trial-and-error approach discussed in Section III.5, is used, good agreement in all energy groups is found. The stationary spectrum obtained by integrating all time-dependent spectra was less sensitive to cross section changes. Nevertheless better agreement was obtained with the ADJUSTED set, as shown in Fig. 12. The relative group changes applied to the original KEDAK data are illustrated at the top of this figure. The inelastic scattering cross section data from KEDAK and the smoothed ADJUSTED data are shown in Fig. 13.

IV.2 Results of the uranium assembly

In the calculation of the uranium assembly three inelastic scattering cross section data were used: KEDAK, BLUHM /33/ and the ADJUSTED. It is shown in Figs. 14 and 15, for the time-dependent spectra, and in Fig. 16, for the stationary spectra, that with the ADJUSTED data closer agreement with the measurements is obtained. The relative group cross section changes with respect to the KEDAK data are shown at the top of Fig. 16. The inelastic cross section data from KEDAK and BLUHM and the smoothed ADJUSTED data are shown in Fig. 17.

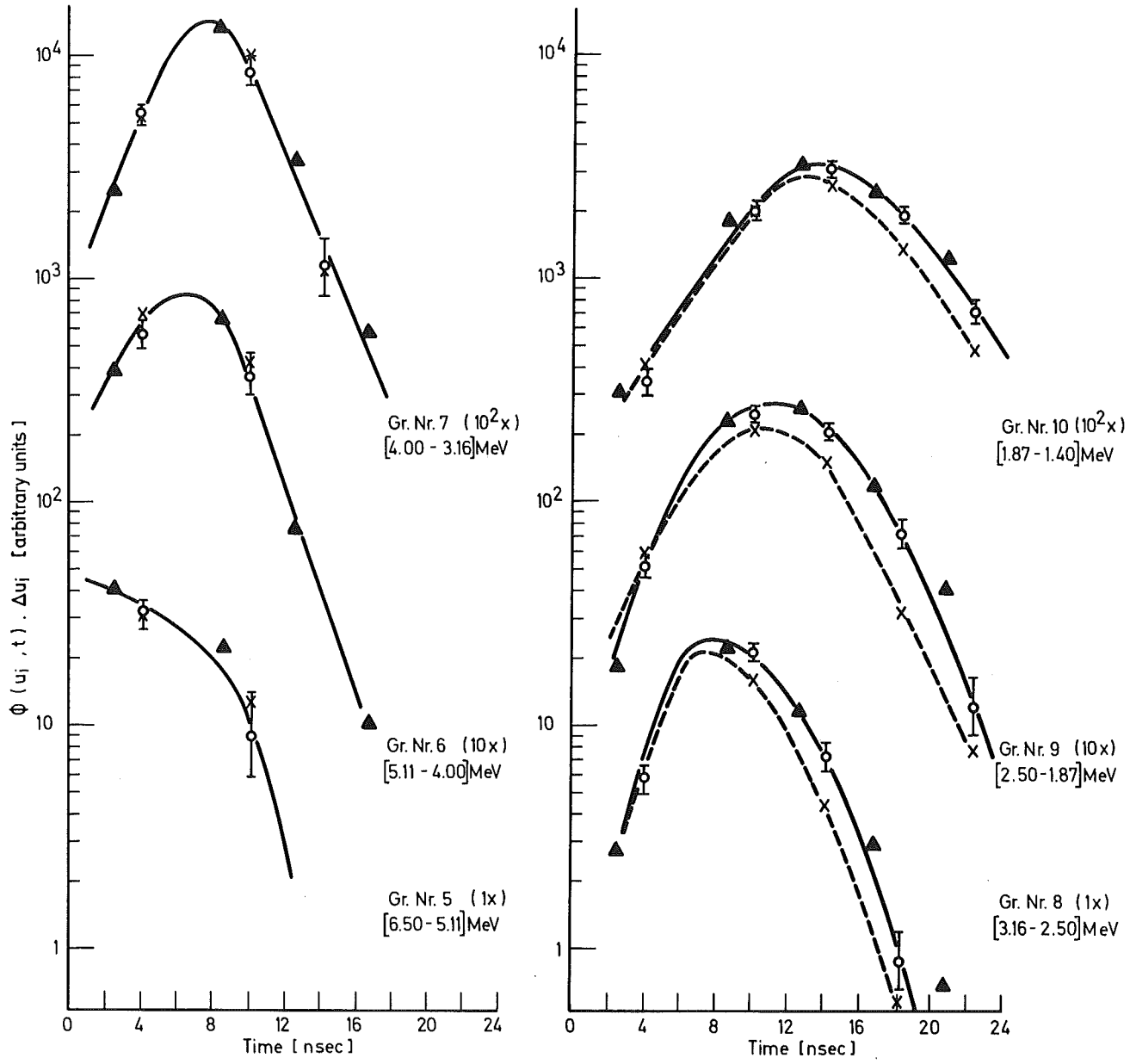

Fig. 10 Measured and Calculated Time-dependent Group Fluxes of the Iron Cylinder ZYLFE 3020

Measurement : ▲

Monte-Carlo Calculation : x KEDAK-SET ---

o ADJUSTED-SET ——

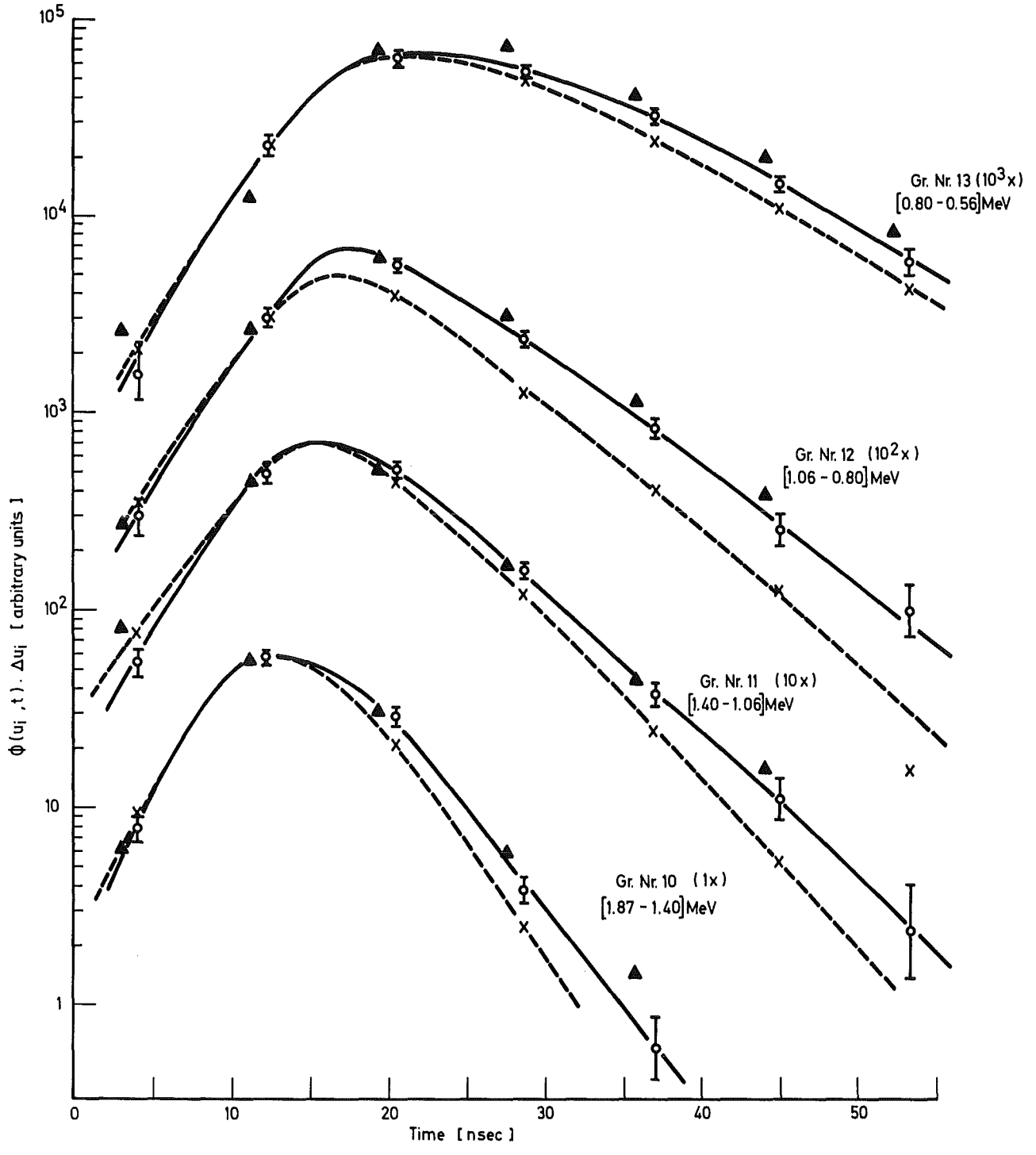

Fig. 11 Measured and Calculated Time - dependent Group Fluxes of the Iron Cylinder ZYLFE 3020

Measurement : ▲

Monte-Carlo Calculation : x KEDAK - SET ---

o ADJUSTED - SET ——

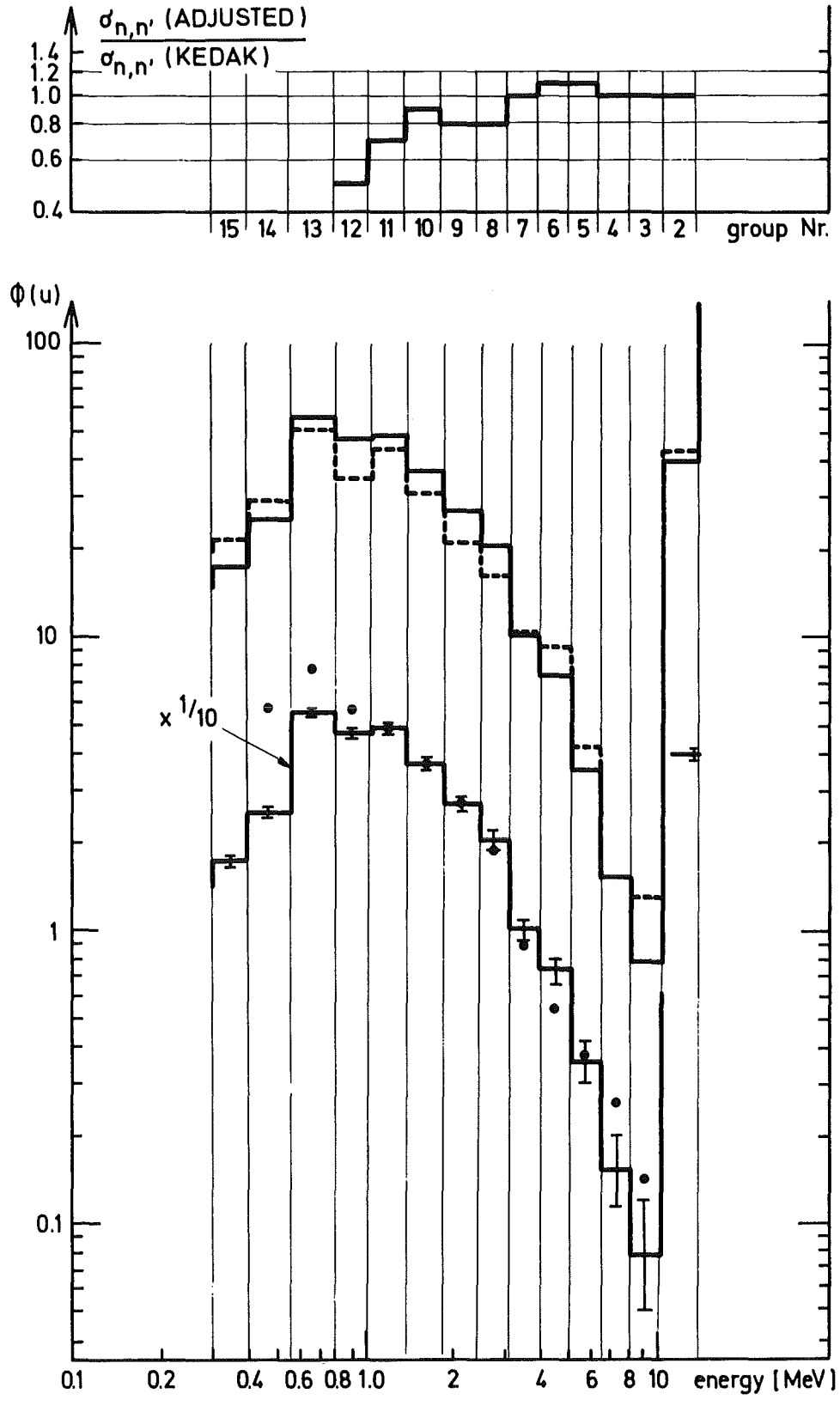

Fig. 12 Measured and Calculated Leakage Spectra of the Iron Cylinder ZYLFE 3020

Measured Spectrum: • NE 213 Scintillator in pulse height mode

Monte-Carlo Calculations: {--- KEDAK - SET
{— ADJUSTED - SET

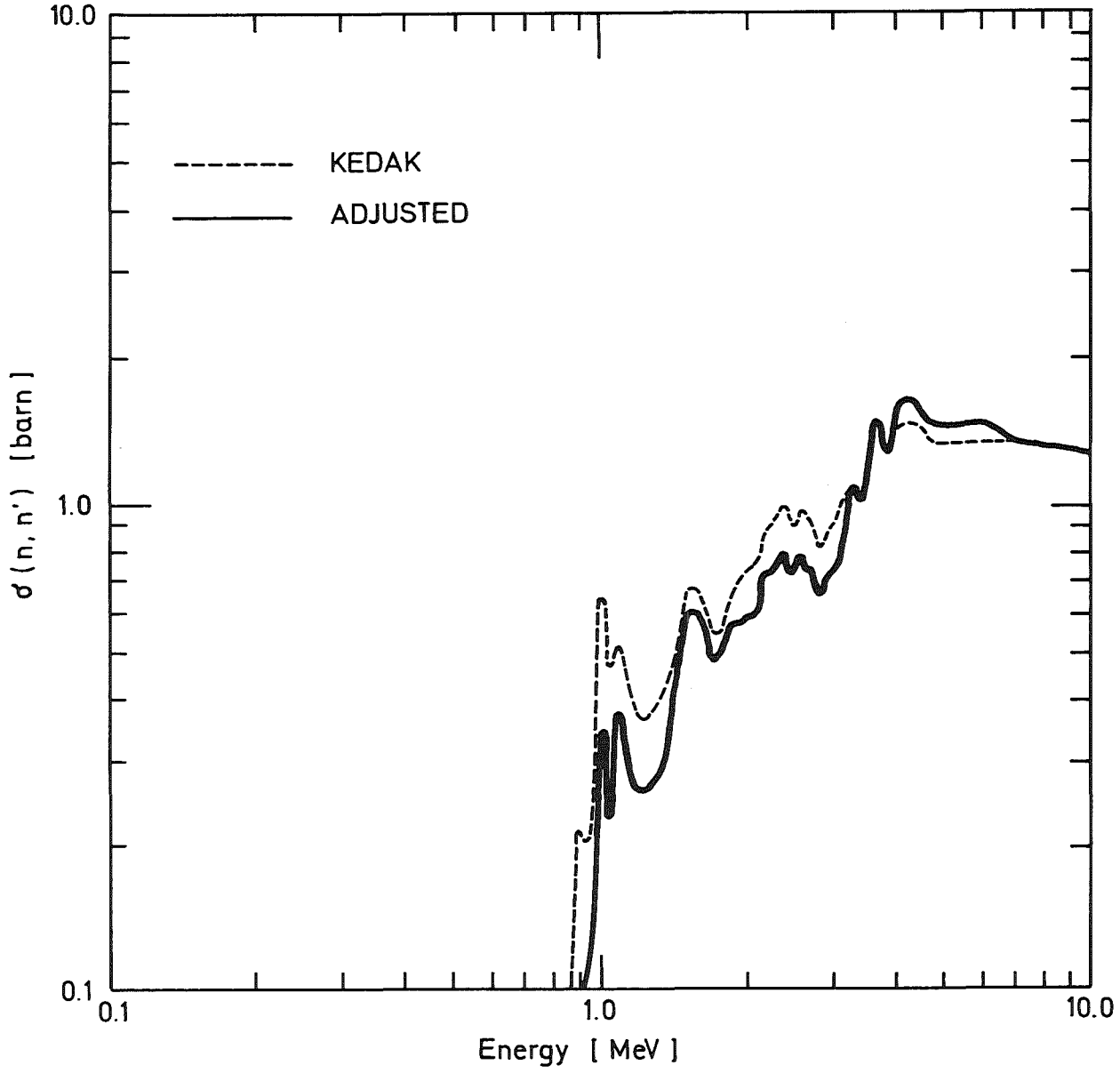

Fig.13 Inelastic Scattering Cross Sections for Iron

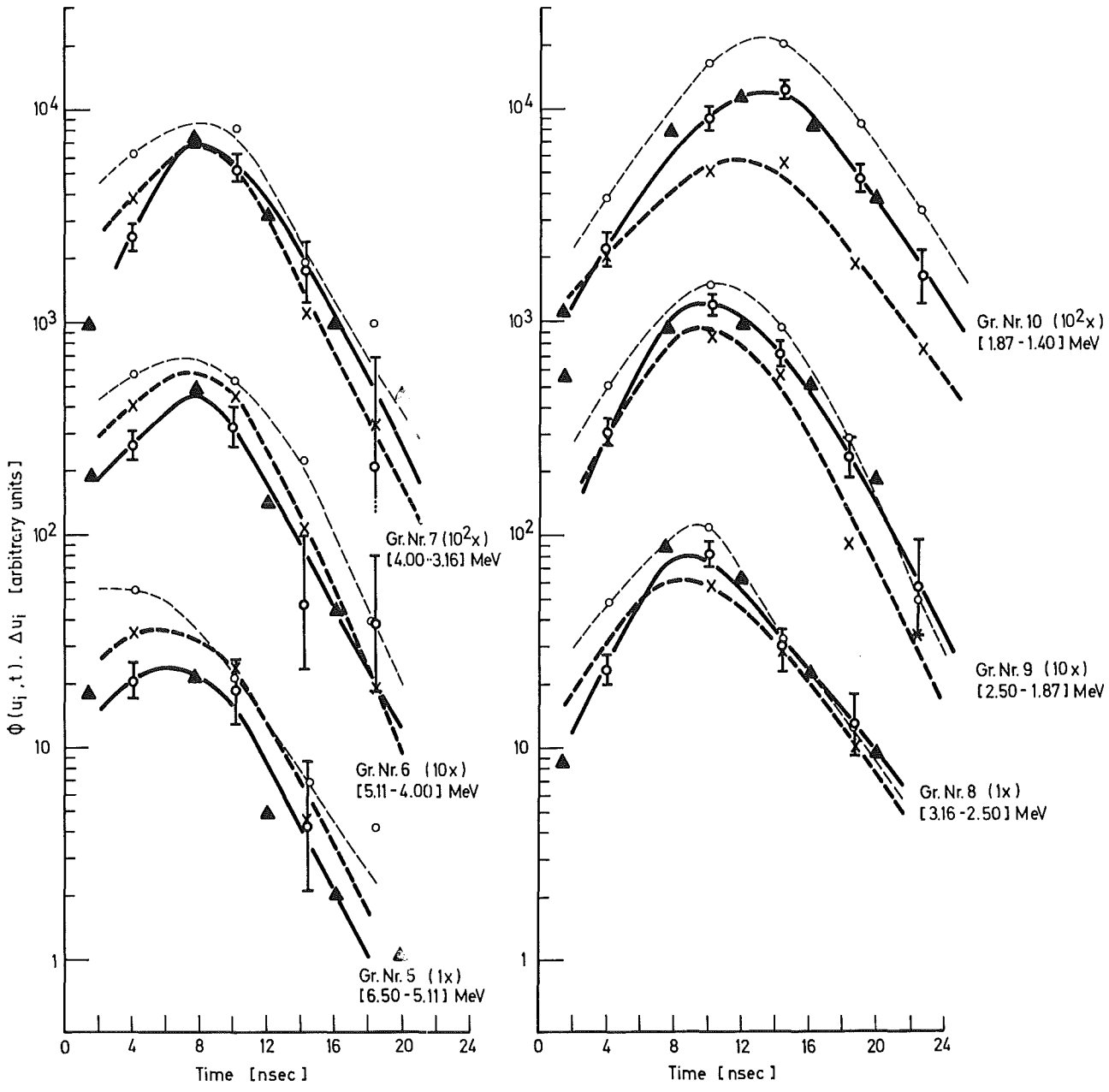

Fig. 14 Measured and Calculated Time-dependent Group Fluxes of the Natural Uranium Cylinder ZYLU 3020

Measurement: ▲

Monte-Carlo Calculation:
x KEDAK - SET ———
o BLUHM - SET – – –
o ADJUSTED - SET ——

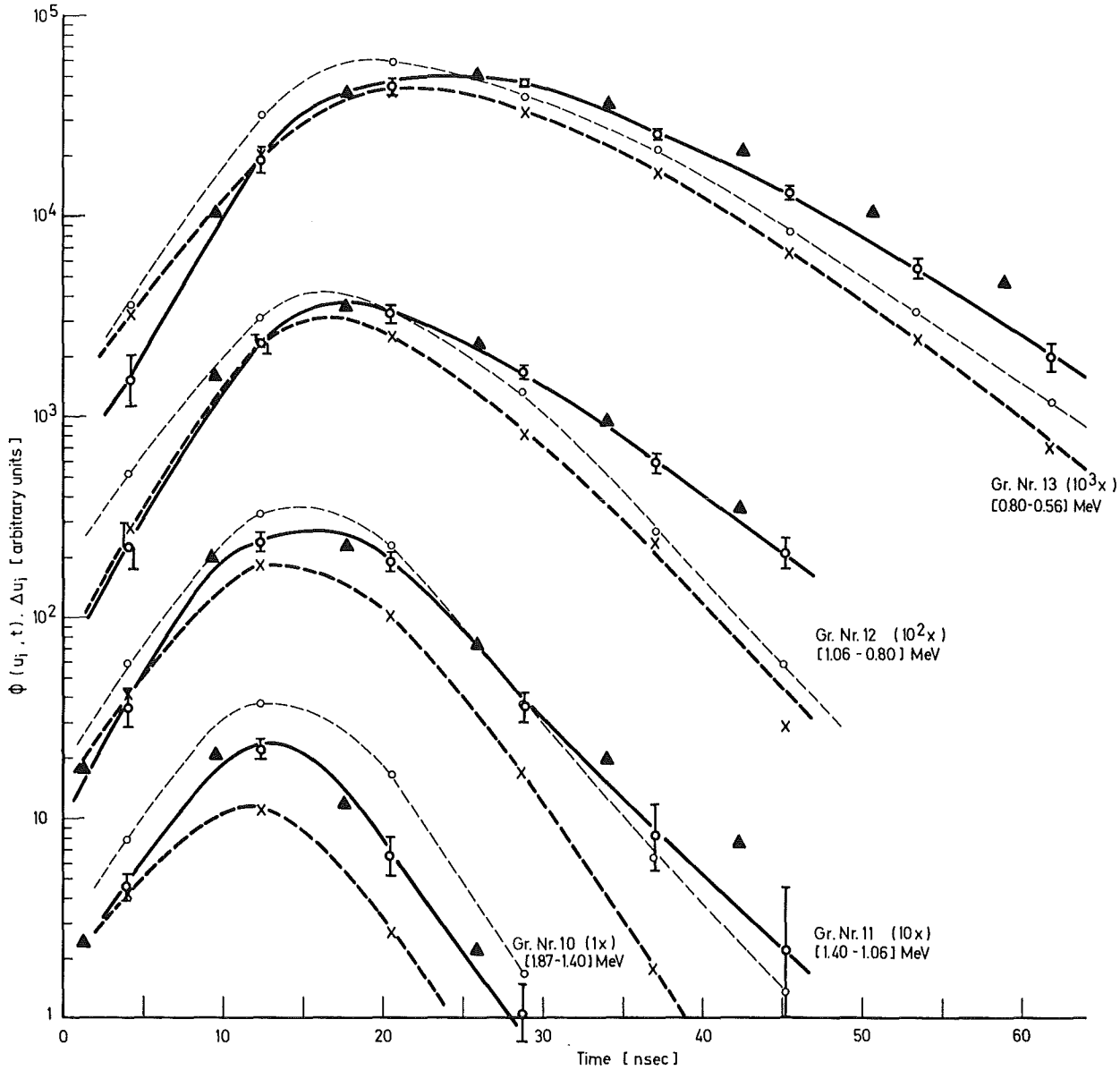

Fig. 15 Measured and Calculated Time-dependent Group Fluxes of the Natural Uranium Cylinder ZYLU 3020

Measurement : ▲

Monte-Carlo Calculation : x KEDAK-SET ---
o BLUHM-SET - - -
o ADJUSTED-SET ——

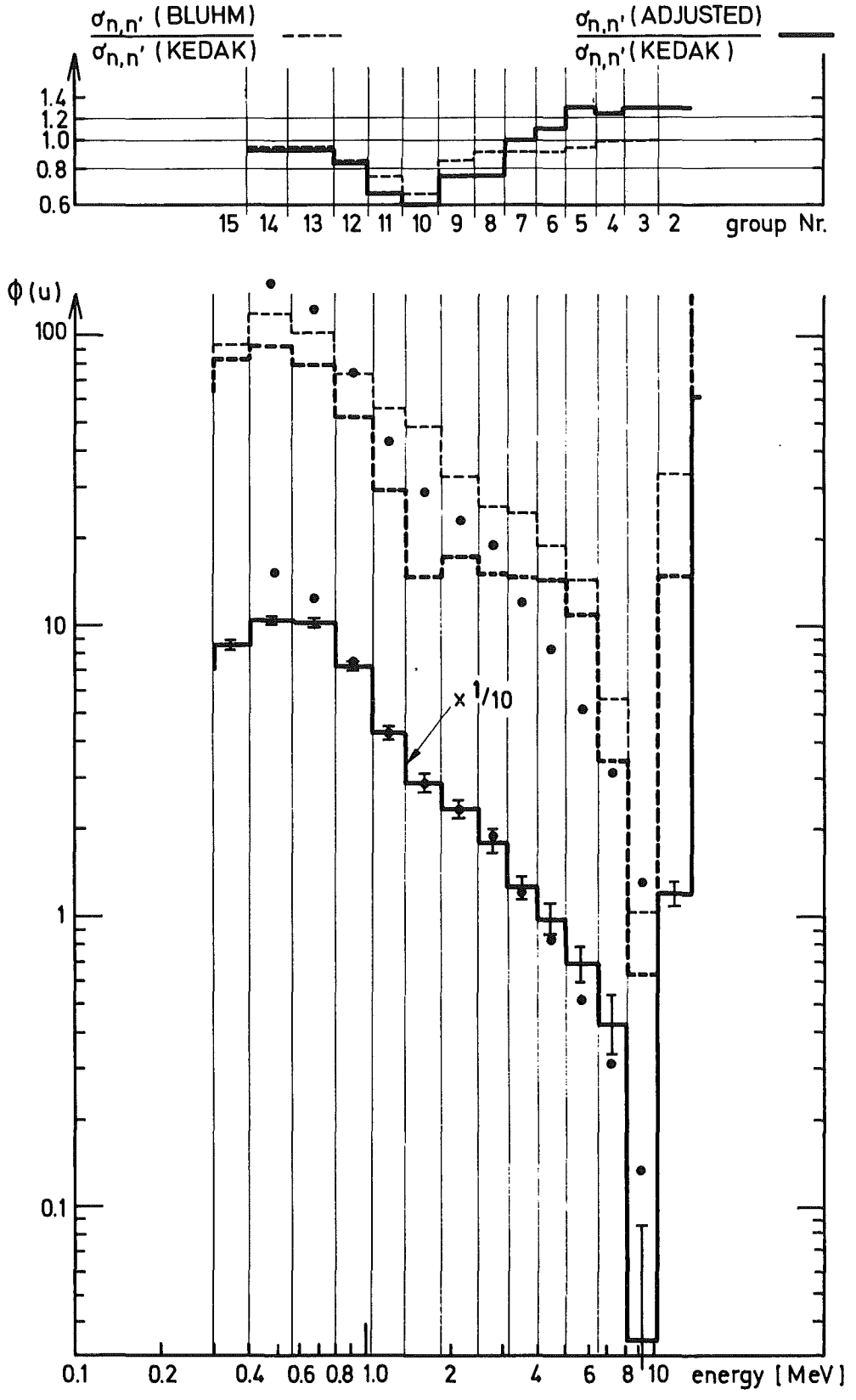

Fig. 16 Measured and Calculated Leakage Spectra of the Natural Uranium Cylinder ZYLU 3020

Measured Spectrum : • NE 213 Scintillator in pulse height mode

Monte-Carlo Calculations: KEDAK - SET; BLUHM - SET; ADJUSTED - SET

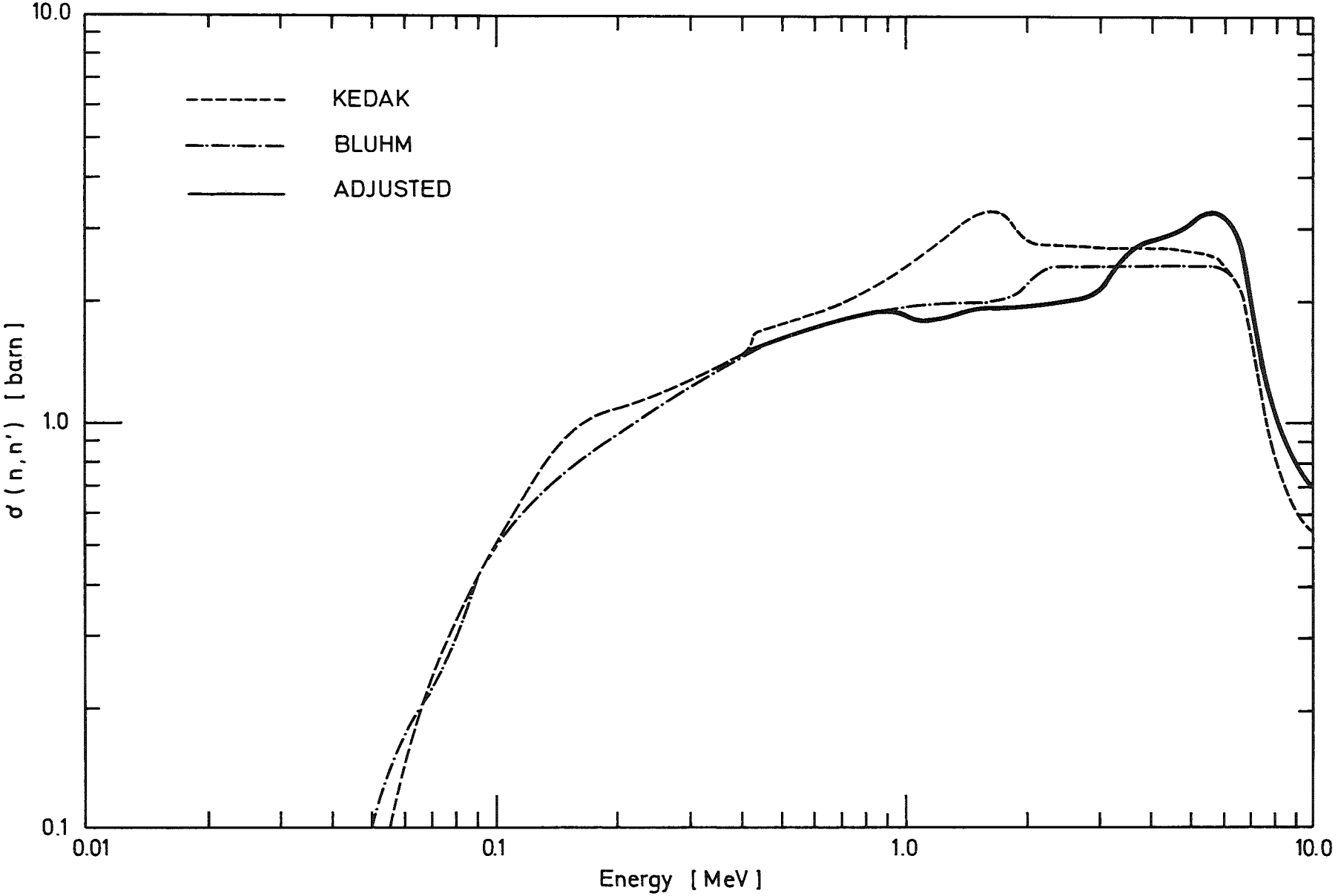

Fig.17 Inelastic Scattering Cross Sections for ^{238}U

Chapter V

VERIFICATION OF THE ADJUSTED DATA

To verify the reliability of the ADJUSTED inelastic scattering cross section data defined in this study, they were applied in the calculation of independent experiments.

V.1 Iron assembly with a californium source

The stationary leakage spectra through a flat face of an iron cylinder, 15.0 cm radius and 15.0 cm height, with a ^{252}Cf source placed at the opposite face, was measured.
The KAMCCO program was used for a census time of 50 nsec, which is enough to describe the stationary spectra above 400 KeV /34/. The exact geometry of the system, including the detector, was taken into account. A calculation time of about 60 minutes was needed to obtain accuracies between 3 and 15 % in the energy groups below 4 MeV. To obtain a similar accuracy for the energy groups above 4 MeV, another 20 minute KAMCCO calculation was performed in which a truncation of the californium source spectrum below 4 MeV was applied.
The calculations were performed with the KEDAK data for the inelastic cross section, and with the ADJUSTED data. As shown in Fig. 18, the ADJUSTED data provide better agreement with the measurement.

V.2 Fast critical uranium assembly

The assembly SNEAK-8 was an uranium core with a k_∞ test zone /35/. The integral parameters of this core are sensitive to the proprieties of ^{238}U. For the calculations the KAPER program /36/ was used, which is a multigroup lattice program routinarily used to analyze experiments performed in SNEAK-type critical facilities.

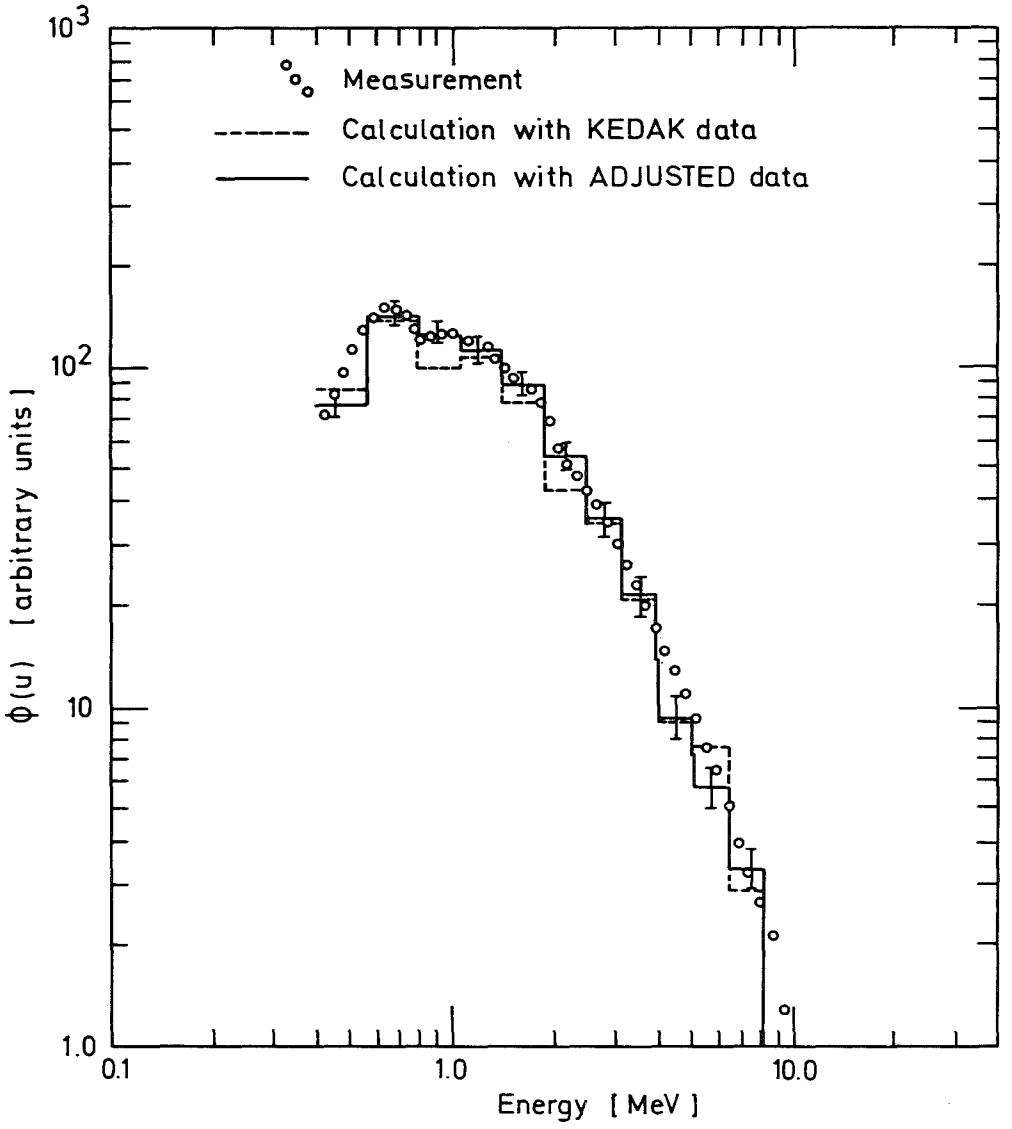

Fig.18 Leakage Stationary Spectra of an Iron Assembly with a Californium Source

A first calculation was performed using the KFKINR set of group cross section data /37/. The weighting function inherent in the KFKINR set was applied to generate group inelastic scattering cross sections from the KEDAK and the ADJUSTED sets for ^{238}U. The group data is given in Table IV. The new data replaced the inelastic cross section data of the KFKINR set in the KAPER calculations. The results of these calculations for the infinite multiplication factor k_∞ and the ratios of ^{238}U capture and fission to ^{235}U fission are presented in Table V, together with measured results. It is seen that the results obtained with the ADJUSTED set agree better with the measurements than those obtained with the KEDAK set. In addition, the results with the ADJUSTED set also agree with those obtained with the KFKINR set. A similar agreement between results obtained with the ADJUSTED set and with the KFKINR set was found in a calculation of about 30 fast zero power cores /38/. It is worthwhile to mention that the KFKINR data set was obtained by a completely independent evaluation method.

The agreement obtained with the ADJUSTED data for iron and ^{238}U verifies the ability of the present method to define reliable corrections to the total inelastic scattering cross section data.

Table IV

Group inelastic scattering cross sections for ^{238}U

Group	Upper Energy MeV	Group inelastic cross section (barn) KFKINR Set	KEDAK SET	ADJUSTED Set
1	10.5	1.16	1.25	1.68
2	6.5	2.10	2.56	2.95
3	4.0	2.25	2.61	2.18
4	2.5	2.25	2.79	1.93
5	1.4	2.15	2.67	1.83
6	0.8	1.60	1.74	1.65
7	0.4	1.05	1.08	1.08
8	0.2	0.65	0.77	0.77
9	0.1	0.25	0.21	0.21

Table V

Fast reactor parameter calculation for SNEAK-8 core with different inelastic scattering cross section data

Inelastic data	Calculation			Measurement
	KFKINR	KEDAK	ADJUSTED	
k_∞	0.9954	0.9625	0.9963	1.0065 ± 0.0018
$\frac{^{238}U \text{ capture}}{^{235}U \text{ fission}}$	0.122	0.123	0.123	0.115 ± 0.003
$\frac{^{238}U \text{ fission}}{^{235}U \text{ fission}}$	0.0226	0.0197	0.0232	0.0222 ± 0.0006

Chapter VI

CONCLUSIONS

A method to test and improve neutron inelastic scattering cross section data of reactor materials has been developed. It is based on the large sensitivity of fast nanosecond decay leakage spectra of small pulsed systems to the inelastic scattering process. By analyzing the decaying spectra in small energy intervals, quantitative changes in the inelastic scattering cross section data can be introduced to achieve agreement between calculation and measurement. In this manner adjusted data can be defined.

The present work provided adjusted data for the total inelastic scattering cross sections of iron and ^{238}U, maintaining the respective inelastic scattering matrixes unaltered. These data were verified through independent experiments, proving the reliability of the information obtained.

The present method can be applied to the investigation of other materials of interest in fast reactors.

Appendix A

TRADI - Code for Unfolding Pulse Height Distributions Measured by an Organic Proton Recoil Detector

Computer Code Abstract

T R A D I

1. Name of Code: TRADI, a code for unfolding pulse height distributions measured by an organic proton recoil detector.

2. Computer for Which Code is Designed: IBM 370/165.
   Programming Language Used: FORTRAN IV.

3. Nature of Physical Problem Solved: The experimental pulse height distribution obtained with a proton recoil detector is unfolded by TRADI to provide the neutron flux.

4. Method of Solution: Transformation of pulse height to recoil proton energy by an analytical fitting of the measured response of the detector to monoenergetic neutrons. With the assumption of a constant energy distribution of the recoil protons, the neutron flux is then obtained by a differentiation of the experimental pulse height distribution.

5. Restrictions on the Complexity of the Problem: The present version of TRADI was developed for an organic scintillator detector. Minor parameter changes are needed when used for other types of proton recoil detectors.

6. Typical Machine Time: 4.8 sec CPU time for a run with 512 pulse height channels.

7. Unusual Features of the Program: It is a very simple and flexible code, that can be easily adapted to the special requirements of the experiment being unfolded.

8. Status: In use.

9. Machine requirements: 104 K-Bytes on IBM 370/165.

10. Operating System or Monitor Under Which Program is Executed: OS 360-370, MVT, Release 20 in connection with ASP.

11. Material Available: (from IASR, Kernforschungszentrum Karlsruhe) FORTRAN Deck, Sample Problem, Sample Problem Results, Instruction Manual.

A.1 Program Flow

A flow diagram of the TRADI code is shown in Fig. a . The operations are performed by several subroutines which are briefly described here. A listing of the program is given in Appendix B.

A.1.1 Subroutine CONVER

This subroutine performs the transformation of the pulse height V to the proton energy E_p according to Eq. (1). It uses as input the coefficients A_i which are obtained from the least squares fitting program LESQU /16/, applied to the detector data. For a NE 213 liquid scintillator detector the data needed are obtained from references /13,15/, or from the present work.

As electronic settings may vary from one experiment to another, a calibration must be applied between the present experimental pulse height scale and the scale originally used to obtain the coefficients A_i. When a 14 MeV neutron source is available, which is frequently the case in most measurements, a convenient calibration can be performed using the measured pulse height for the 14 MeV neutrons, here defined as V_M (14 MeV). The calibration factor CF is defined as

$$CF = \frac{V_A \text{ (14 MeV)}}{V_M \text{ (14 MeV)}}$$

where V_A (14 MeV) is the 14 MeV pulse height from the data used to obtain the A_i coefficients.

Another convenient calibration procedure of the pulse height scale can be obtained with the Compton-edge in a pulse height spectrum of a ^{22}Na-gamma ray source.

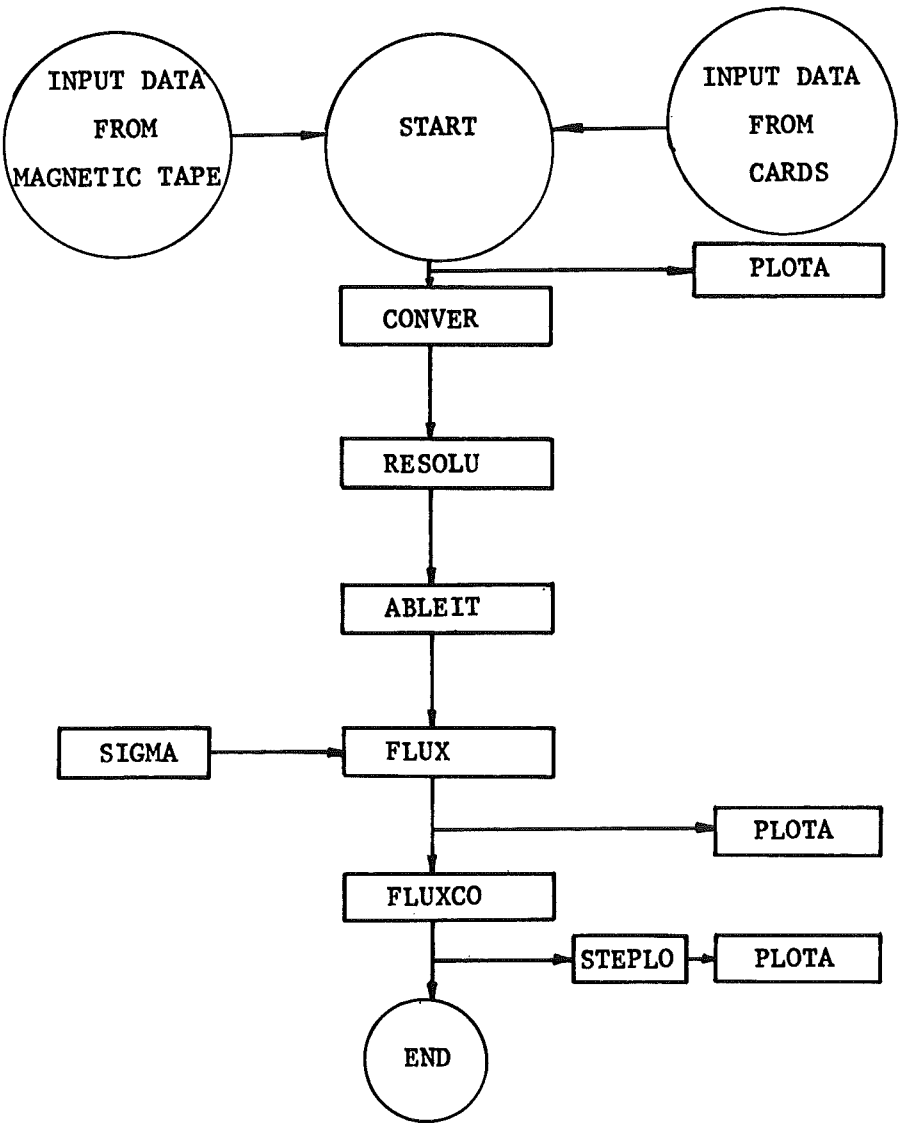

Fig. a: Flow diagram of TRADI

CONVER determines the energy corresponding to the midpoint of each experimental channel. In the midpoint of the first channel is $V = E_p = 0$.

A.1.2 Subroutine RESOLU

The channel width in a normal multichannel analyzer remains constant during each measurement. To have a constant resolution of the measured pulse height distribution, the subroutine RESOLU performs a combination by adding the channel count numbers so that $\Delta V/V$ is held approximately constant and equal to or less than the given intrinsic resolution of the spectrometer. This pulse height distribution per combined group width, $N(V)$, is then transformed to the proton energy distribution $P(E_p)$, per unit energy, using the data provided by the subroutine CONVER.

A.1.3 Subroutine ABLEIT

The subroutine ABLEIT /39/ fits a second order polynomial to the proton energy distribution $P(E_p)$. In order to smooth the experimental statistical fluctuations, a given number of channels is grouped together prior to the fitting. The derivative $\frac{d}{dE_p} P(E_p)$ is deduced from the coefficients of the polynomial fitting.

A.1.4 Subroutine FLUX

This subroutine determines the flux with the relation as given in Eq. (16). The subroutine FLUX provides the flux per unit energy and unit lethargy corresponding to the midpoint of the combined channels.

A.1.5 Subroutine FLUXCO

FLUXCO performs a flux condensation of a given number of energy groups. This is done by taking the arithmetic mean value of the obtained point fluxes between the boundaries of each group. As energy group boundaries do not necessarily coincide with channel boundaries, the flux at the group boundaries is determined by linear interpolation.

A.1.6 Function SIGMA

The analytical value of $\sigma_H(E_n)$ according to Eq. (14) is calculated by this subprogram and transferred to the FLUX subroutine.

A.1.7 Subroutine STEPLO

The condensed flux values from the subroutine FLUXCO are arranged so as to give a suitable input for a histogram plot in the subroutine PLOTA.

A.1.8 Subroutine PLOTA

The optional plotting of channel count number vs. channel number, flux per lethargy unit vs. energy, and condensed flux per lethargy unit vs. energy are performed by the subroutine PLOTA /40/.

A.2 Input Data

The input consists of: 1) data related to the measuring system used, given on cards, and 2) the channel count numbers registered in a Multichannel Analyzer, which are read from a magnetic tape.

The following card descriptions are given in the order in which they must appear in the data deck. Standard FORTRAN conventions relating type and name of the variable are used.

Card 1 : (2F7.6,2F4.2)

AH = H-Atoms $[10^{+24}/cm^3]$

AC = C-Atoms $[10^{+24}/cm^3]$

DIR = detector radius [cm]

DIL = detector length [cm]

Card 2 : (I3,F6.3)

KM = number of condensed energy groups ($\leq$30)

EU = energy [MeV] for which the lethargy is zero

Card 3 : (10F7.4)

(EC(K),K=1,KM) = upper energy boundaries [MeV] of the KM condensed groups (lower boundary for the last group is 0)

Card 4 : (6F10.8)

(AI(I),I=1,6) = coefficients for the transformation in Eq. (1). See Section II.2.1 .

Card 5 : (6I2,I4)

KD = number corresponding to the day of measurement

M = number corresponding to the month of measurement

KYE = last two numbers corresponding to the year of the measurement

NM = identification number of the measurement

NU = number of the external unit from where the data from the magnetic tape are to be read

LI = number of channels plus one in Y-direction from previous measurements recorded on the same label of the input magnetic tape

LY = number of channels in Y-direction. For a one dimensional measurement LY = 1.

Card 6 : (F4.3,2I4)

ES = threshold energy [MeV] of the detection system

IANF = channel in which the unfolding is initiated

IFIT = number of channels to be grouped for smoothing in the second order polynomial fitting and differentiation. IFIT = 2n+1, n=1,2,3,.....

Card 7 : (F3.3,F6.3)

RESU = resolution $\frac{\Delta V}{V}$ of the detection system

CF = calibration factor for the pulse height - proton energy transformation. See Section A.1.1 .

Card 8 : (3I2)

LCN = 1:plot of experimental count number vs. channel-number
0:no plot

LUF = 1:plot of flux per lethargy unit vs. energy
0:no plot

LGF = 1:plot of group flux per lethargy unit vs. energy
0:no plot

Card 9 : (15A4)

IDENT = identification title to be printed in the output

IF LCN=1, extra Card: (15A4)

IDCN = identification title to be printed in the plot of experimental count number vs. channel number

IF LUF=1, extra Card (15A4)

IDUF = identification title to be printed in the plot of flux per lethargy unit vs. energy

IF LGF=1, extra Card (15A4)

IDGF = identification title to be printed in the plot of group flux per lethargy unit vs. energy

If another experience must be unfold, add the corresponding data starting from Card 5. If no more experiences,add 1 blank card.

The following data are to be read from a magnetic tape:

IENDE, (T(I),I=1,IENDE)

IENDE = number of channels in X-direction (or number of channels in a monodimensional measurement)

T(I) = count number in channel I

See Appendix B for details concerning preparation of magnetic tape.

A.3 Program output

The printed output of TRADI is

- identification title and run number of the experiment unfolded
- detection system data given as input
- experimental channel count number

- combined count number ($\Delta V/V \simeq$ constant)
- mean energy and mean lethargy for the midpoint of the combined channels
- flux per unit energy and flux per unit lethargy for the midpoint of the combined channels
- condensated fluxes per unit energy, per unit lethargy, and integrated fluxes for the energy groups given in input

Optionally the experimental count number vs. channel number, flux per unit lethargy vs. energy and group flux per unit lethargy vs. energy are plotted.

A.4 Sample Problem

The stationary neutron spectrum of a Californium source is unfolded from the measured pulse height distribution.

DATA	INPUT DATA
A NE 213 organic liquid scintillator detector was used, with the following characteristics:	
$N_H = 0.048763 \times 10^{24}$ at/cm^3	AH = 0.048763
$N_C = 0.040200 \times 10^{24}$ at/cm^3	AC = 0.040200
R = 2.54 cm	DIR = 2.54
L = 5.08 cm	DIL = 5.08
It is desired to condense the flux to 16 energy groups.	KM = 16
Lethargy zero at energy 28.54 MeV	EU = 28.54
The group upper energy limits must be (in MeV): 14.1 - 14.0 - 10.5 - 8.25 - 6.5 - 5.11 - 4.0 - 3.16 - 2.5 - 1.87 - 1.4 - 1.058 - 0.8 - 0.565 - 0.4 - 0.2828	EC(K),K=1,16

DATA	INPUT DATA
The coefficients A_i obtained by the subroutine LESQU /14/ applied to the data obtained for this detector at SUAK are (Table I) A_1 = -1.57761955 A_2 = 0.32292497 A_3 = 0.26951498 A_4 = -0.07669628 A_5 = 0.00476279 A_6 = 0.00064185	AI(I),I=1,6
The measurement was performed on August 13, 1972	KD = 13 M = 8 KYE = 72
The run was asigned the number 2.	NM = 2
The magnetic tape is to be read from unit 8.	NU = 8
A previous monodimensional measurement was recorded under the same label on the magnetic tape.	LI = 2
The present is a monodimensional measurement.	LY = 1
The threshold energy of the detection system is 250 keV.	ES = 0.250
The number of the channel in which the unfolding is initiated, is 15.	IANF = 15
The number of channels to be grouped for fitting is 5.	IFIT = 5

DATA	INPUT DATA
The resolution of the system is 4%.	RESU = 0.04
The pulse height corresponding to 14 MeV neutron from the measurement used to obtain the A_i coefficients and that from the present measurement give from Eq. (17) CF = 35.030	CF = 35.030
Plot of experimental count number vs. channel number is desired.	LCN = 1
Plot of flux pro lethargy unit vs. energy is desired.	LUF = 1
Plot of group flux pro lethargy unit vs. energy is desired.	LGF = 1

The data prepared for punching on cards are given in Table A.

The measured count number stored in the multichannel analyzer is provided by a punched tape. In Appendix C a procedure is given for transfering this data to a magnetic tape to be used as input for TRADI.

In Table B the output of the program for this sample problem is shown. The CPU time needed was 4.83 sec.

DATENKARTEN

Programm TRADI Datum 19.12.72 Name Pieroni Blatt-Nr. 1

Table A. Input data for the sample problem

```
48763 40200 254 508
16 28510
141000 140000 105000 82500 65000 51100 40000 31600 25000 18700
14000 10580 8000 5650 4000 2828
-1577 61955 32292497 26951498- 7669628 476279 64185
13 872 2 8 2 1
250 15 5
40 35030
1 1 1
CALIFORNIUM NEUTRON SPECTRUM MEASURED WITH A NE-213 DETECTOR
CALIFORNIUM MEASUREMENT * COUNT-NUMBER VS. CHANNEL-NUMBER
CALIFORNIUM MEASUREMENT * UNITARY FLUX VS. ENERGY (MEV)
CALIFORNIUM MEASUREMENT * GROUP FLUX VS. ENERGY (MEV)
```

— Blank card —

ENERGY SPECTRUM FROM A PULSE-HEIGHT DISTRIBUTION

CALIFORNIUM NEUTRON SPECTRUM MEASURED WITH A NE-213 DETECTOR

RUN 13. 8.72. 2 Y-CHANNEL = 1

THRESHOLD ENERGY = 0.250 MEV

INITIAL CHANNEL IANF = 15

GROUPED CHANNELS IFIT = 5

PULSE HEIGHT RESOLUTION = 0.040

CALIBRATION FACTOR CF = 35.030

TRANSFORMATION COEFFICIENTS :

A(1) = -1.57761955
A(2) = 0.32292497
A(3) = 0.26951498
A(4) = -0.07669628
A(5) = 0.00476279
A(6) = 0.00064185

H-ATOMS = 0.048763E 24 1/CM3
C-ATOMS = 0.040200E 24 1/CM3

DETECTOR-RADIUS = 2.54 CM
DETECTOR-LENGHT = 5.08 CM

Table B Output for the sample problem

ENERGY SPECTRUM FROM A PULSE-HEIGHT DISTRIBUTION

CALIFORNIUM NEUTRON SPECTRUM MEASURED WITH A NE-213 DETECTOR

RUN 13. 8.72. 2 Y-CHANNEL = 1

EXPERIMENTAL PULSE-HEIGHT DISTRIBUTION

1	69999.	2	0.	3	0.	4	0.	5	0.	6	3.	7	1010.	8	85932.	9	764676.
10	714687.	11	640116.	12	572909.	13	514961.	14	466194.	15	424399.	16	387806.	17	357588.	18	329164.
19	308011.	20	286707.	21	267643.	22	249453.	23	235071.	24	219011.	25	205727.	26	192235.	27	182511.
28	172562.	29	162569.	30	153827.	31	145505.	32	137656.	33	130826.	34	123256.	35	117626.	36	111665.
37	105933.	38	101351.	39	96355.	40	91131.	41	87359.	42	83247.	43	78895.	44	75695.	45	72398.
46	68570.	47	65966.	48	62862.	49	59837.	50	57445.	51	55306.	52	52491.	53	50380.	54	48604.
55	46067.	56	44515.	57	42450.	58	40920.	59	39331.	60	38140.	61	36402.	62	34662.	63	33753.
64	32475.	65	31192.	66	30051.	67	28878.	68	27774.	69	26837.	70	25894.	71	24981.	72	24066.
73	23431.	74	22296.	75	21675.	76	21107.	77	20420.	78	19596.	79	18816.	80	18428.	81	17759.
82	17041.	83	16792.	84	16051.	85	15285.	86	15152.	87	14641.	88	14122.	89	13679.	90	13265.
91	12955.	92	12664.	93	12010.	94	11887.	95	11186.	96	11034.	97	10640.	98	10188.	99	9863.
100	9518.	101	9244.	102	9153.	103	8856.	104	8526.	105	8248.	106	8086.	107	7778.	108	7599.
109	7187.	110	7437.	111	7012.	112	6698.	113	6409.	114	6243.	115	6191.	116	5936.	117	5830.
118	5545.	119	5336.	120	5447.	121	5134.	122	4981.	123	4818.	124	4695.	125	4561.	126	4338.
127	4328.	128	4123.	129	4061.	130	3916.	131	3793.	132	3735.	133	3662.	134	3550.	135	3350.
136	3335.	137	3195.	138	3119.	139	3010.	140	2954.	141	2918.	142	2812.	143	2746.	144	2642.
145	2608.	146	2579.	147	2455.	148	2329.	149	2259.	150	2274.	151	2164.	152	2079.	153	2030.
154	1985.	155	2004.	156	1869.	157	1829.	158	1806.	159	1715.	160	1675.	161	1667.	162	1560.
163	1531.	164	1501.	165	1449.	166	1472.	167	1422.	168	1446.	169	1321.	170	1256.	171	1226.
172	1181.	173	1161.	174	1115.	175	1167.	176	1093.	177	1038.	178	1032.	179	1012.	180	1020.
181	978.	182	956.	183	933.	184	895.	185	849.	186	865.	187	810.	188	835.	189	816.
190	752.	191	761.	192	708.	193	704.	194	680.	195	670.	196	638.	197	661.	198	629.
199	562.	200	573.	201	551.	202	523.	203	549.	204	537.	205	480.	206	491.	207	541.
208	447.	209	532.	210	439.	211	454.	212	418.	213	407.	214	420.	215	391.	216	427.
217	358.	218	382.	219	370.	220	382.	221	323.	222	344.	223	306.	224	317.	225	282.
226	311.	227	285.	228	287.	229	285.	230	262.	231	301.	232	275.	233	302.	234	232.
235	255.	236	210.	237	101.	238	0.	239	0.	240	0.	241	0.	242	0.	243	0.
244	1.	245	0.	246	0.	247	0.	248	0.	249	0.	250	0.	251	2.	252	0.
253	0.	254	0.	255	0.	256	0.	257	0.	258	0.	259	0.	260	0.	261	0.
262	0.	263	0.	264	0.	265	0.	266	0.	267	0.	268	0.	269	0.	270	0.
271	0.	272	0.	273	0.	274	0.	275	0.	276	0.	277	0.	278	0.	279	0.
280	0.	281	0.	282	0.	283	0.	284	0.	285	0.	286	0.	287	0.	288	0.
289	0.	290	0.	291	0.	292	0.	293	0.	294	0.	295	0.	296	0.	297	0
298	0.	299	0.	300	0.	301	0.	302	0.	303	0.	304	0.	305	0.	306	0.
307	0.	308	0.	309	1.	310	0.	311	0.	312	1.	313	0.	314	0.	315	0.
316	0.	317	0.	318	0.	319	0.	320	0.	321	0.	322	0.	323	0.	324	0.
325	1.	326	0.	327	1.	328	0.	329	0.	330	0.	331	0.	332	0.	333	0.
334	1.	335	0.	336	1.	337	1.	338	0.	339	0.	340	0.	341	0.	342	0.
343	0.	344	0.	345	0.	346	0.	347	0.	348	0.	349	0.	350	0.	351	0.
352	0.	353	0.	354	0.	355	0.	356	1.	357	0.	358	0.	359	0.	360	0.
361	0.	362	0.	363	0.	364	0.	365	0.	366	0.	367	0.	368	0.	369	0.
370	0.	371	0.	372	0.	373	0.	374	0.	375	0.	376	0.	377	0.	378	0.
379	0.	380	0.	381	0.	382	0.	383	0.	384	0.	385	0.	386	0.	387	0.
388	0.	389	0.	390	0.	391	0.	392	0.	393	0.	394	0.	395	0.	396	0.
397	0.	398	0.	399	0.	400	0.	401	0.	402	0.	403	0.	404	0.	405	0.
406	0.	407	0.	408	0.	409	0.	410	0.	411	0.	412	0.	413	0.	414	0.
415	0.	416	0.	417	0.	418	0.	419	0.	420	0.	421	0.	422	0.	423	0.
424	0.	425	0.	426	0.	427	0.	428	0.	429	0.	430	0.	431	0.	432	0.
433	0.	434	0.	435	0.	436	0.	437	0.	438	0.	439	0.	440	0.	441	0.
442	0.	443	0.	444	0.	445	0.	446	0.	447	0.	448	0.	449	0.	450	0.
451	0.	452	0.	453	0.	454	0.	455	0.	456	0.	457	0.	458	0.	459	0.
460	0.	461	0.	462	0.	463	0.	464	0.	465	0.	466	0.	467	0.	468	0.
469	0.	470	0.	471	0.	472	0.	473	0.	474	0.	475	0.	476	0.	477	0.
478	0.	479	0.	480	0.	481	0.	482	0.	483	0.	484	0.	485	0.	486	0.
487	0.	488	0.	489	0.	490	0.	491	0.	492	0.	493	0.	494	0.	495	0.
496	0.	497	0.	498	0.	499	0.	500	0.	501	0.	502	0.	503	0.	504	0.
505	0.	506	0.	507	0.	508	0.	509	0.	510	0.	511	0.	512	0.		

Table B (Continuation)

ENERGY SPECTRUM FROM A PULSE-HEIGHT DISTRIBUTION

CALIFORNIUM NEUTRON SPECTRUM MEASURED WITH A NE-213 DETECTOR

RUN 13. 6.72. 2 Y-CHANNEL = 1

Table B (Continuation)

CHANNEL (COMB.)	COUNT NUMBER (COMBINED)	MEAN ENERGY (MEV)	UNITARY FLUX (ENERGY)	UNITARY FLUX (LETHARGY)	MEAN LETHARGY (U=0 FOR 28.54 MEV)
15	0.42439900E+06	0.12261467E+01	0.84838869E+06	0.10402489E+07	0.31474295E+01
16	0.38780600E+06	0.12820597E+01	0.81166950E+06	0.10406087E+07	0.31028385E+01
17	0.35758800E+06	0.13365889E+01	0.76661725E+06	0.10246521E+07	0.30611849E+01
18	0.32916400E+06	0.13898592E+01	0.73195756E+06	0.10173179E+07	0.30221033E+01
19	0.30801100E+06	0.14415775E+01	0.71449875E+06	0.10302911E+07	0.29852905E+01
20	0.28670700E+06	0.14930363E+01	0.71087881E+06	0.10613670E+07	0.29504938E+01
21	0.26764300E+06	0.15431166E+01	0.71592844E+06	0.11047610E+07	0.29175014E+01
22	0.24945300E+06	0.15922909E+01	0.72147994E+06	0.11488050E+07	0.28861313E+01
23	0.23507100E+06	0.16406231E+01	0.72331931E+06	0.11866940E+07	0.28562298E+01
24	0.21901100E+06	0.16881704E+01	0.73640194E+06	0.12431710E+07	0.28276606E+01
25	0.20572700E+06	0.17349834E+01	0.72618519E+06	0.12599190E+07	0.28003073E+01
26	0.19223500E+06	0.17811079E+01	0.67940050E+06	0.12100850E+07	0.27740707E+01
27	0.18251100E+06	0.18265867E+01	0.66457581E+06	0.12139050E+07	0.27488575E+01
28	0.17256200E+06	0.18714571E+01	0.64861519E+06	0.12138550E+07	0.27245884E+01
29	0.16256900E+06	0.19157543E+01	0.66880425E+06	0.12812640E+07	0.27011948E+01
30	0.15382700E+06	0.19595089E+01	0.66851087E+06	0.13099530E+07	0.26786118E+01
31	0.14550500E+06	0.20027504E+01	0.64880312E+06	0.12993900E+07	0.26567850E+01
32	0.13765600E+06	0.20455046E+01	0.65898037E+06	0.13479470E+07	0.26356621E+01
33	0.13082600E+06	0.20877972E+01	0.64316562E+06	0.13427990E+07	0.26151962E+01
34	0.12325600E+06	0.21296501E+01	0.63008537E+06	0.13418610E+07	0.25953484E+01
35	0.11762600E+06	0.21710854E+01	0.62642031E+06	0.13600110E+07	0.25760784E+01
36	0.11166500E+06	0.22121210E+01	0.59332100E+06	0.13124970E+07	0.25573540E+01
37	0.10593300E+06	0.22527761E+01	0.60236475E+06	0.13569920E+07	0.25391426E+01
38	0.19770600E+06	0.23130398E+01	0.58914937E+06	0.13627250E+07	0.25127439E+01
39	0.17849000E+06	0.23922672E+01	0.57355925E+06	0.13721060E+07	0.24790649E+01
40	0.16214200E+06	0.24702425E+01	0.56440225E+06	0.13942100E+07	0.24469900E+01
41	0.14809300E+06	0.25470648E+01	0.54412419E+06	0.13859190E+07	0.24163647E+01
42	0.13453600E+06	0.26228209E+01	0.52394350E+06	0.13742090E+07	0.23870554E+01
43	0.12269900E+06	0.26975880E+01	0.51036637E+06	0.13767580E+07	0.23589478E+01
44	0.11275100E+06	0.27714348E+01	0.48494762E+06	0.13440000E+07	0.23319407E+01
45	0.10287100E+06	0.28444262E+01	0.46647437E+06	0.13268510E+07	0.23059444E+01
46	0.94671000E+05	0.29166174E+01	0.44911281E+06	0.13098900E+07	0.22808819E+01
47	0.86965000E+05	0.29880600E+01	0.41792175E+06	0.12487750E+07	0.22566814E+01
48	0.80251000E+05	0.30588007E+01	0.40576062E+06	0.12411400E+07	0.22332830E+01
49	0.74542000E+05	0.31288815E+01	0.38573812E+06	0.12069280E+07	0.22106304E+01
50	0.68415000E+05	0.31983433E+01	0.37400812E+06	0.11962060E+07	0.21886730E+01
51	0.93718000E+05	0.32843237E+01	0.35956525E+06	0.11809280E+07	0.21621456E+01
52	0.83489000E+05	0.33864222E+01	0.33123656E+06	0.11217060E+07	0.21315317E+01
53	0.74941000E+05	0.34873962E+01	0.30992306E+06	0.10808240E+07	0.21021509E+01
54	0.67402000E+05	0.35873356E+01	0.28893081E+06	0.10364917E+07	0.20738964E+01
55	0.61123000E+05	0.36863184E+01	0.27234356E+06	0.10039451E+07	0.20466776E+01
56	0.55003000E+05	0.37844172E+01	0.25940419E+06	0.98169362E+06	0.20204144E+01
57	0.49884000E+05	0.38816957E+01	0.24586456E+06	0.95437137E+06	0.19950342E+01
58	0.45078000E+05	0.39782133E+01	0.22854237E+06	0.90919031E+06	0.19704733E+01
59	0.54021000E+05	0.40895048E+01	0.21624325E+06	0.88441425E+06	0.19427843E+01
60	0.47747000E+05	0.42164955E+01	0.20392231E+06	0.85983750E+06	0.19123020E+01
61	0.41725000E+05	0.43420296E+01	0.19271987E+06	0.83679537E+06	0.18829641E+01
62	0.36771000E+05	0.44665985E+01	0.17590831E+06	0.78571175E+06	0.18546791E+01
63	0.32638000E+05	0.45902863E+01	0.16193344E+06	0.74332081E+06	0.18273640E+01
64	0.29235000E+05	0.47131691E+01	0.15055025E+06	0.70956875E+06	0.18009453E+01
65	0.25541000E+05	0.48353081E+01	0.14221269E+06	0.68764212E+06	0.17753611E+01
66	0.28094000E+05	0.49718855E+01	0.13363412E+06	0.66441406E+06	0.17475061E+01
67	0.24189000E+05	0.51227531E+01	0.11838844E+06	0.60647469E+06	0.17176142E+01
68	0.20766000E+05	0.52727509E+01	0.10878237E+06	0.57358231E+06	0.16887541E+01
69	0.18090000E+05	0.54219694E+01	0.96528750E+05	0.52337587E+06	0.16608467E+01
70	0.15613000E+05	0.55704832E+01	0.87375687E+05	0.48672475E+06	0.16338243E+01
71	0.16305000E+05	0.57331181E+01	0.79773250E+05	0.45734944E+06	0.16050463E+01
72	0.13560000E+05	0.59097824E+01	0.72117812E+05	0.42620056E+06	0.15746965E+01

Table B (Continuation)

73	0.11523000E+05	0.60857410E+01	0.64802375E+05	0.39437044E+06	0.15453577E+01
74	0.96490000E+04	0.62610855E+01	0.56577371E+05	0.35423575E+06	0.15169525E+01
75	0.95920000E+04	0.64504299E+01	0.49232125E+05	0.31756831E+06	0.14871588E+01
76	0.77870000E+04	0.66537600E+01	0.41752895E+05	0.27781369E+06	0.14561243E+01
77	0.66430000E+04	0.68565779E+01	0.37290152E+05	0.25568281E+06	0.14260979E+01
78	0.55470000E+04	0.70589752E+01	0.32325449E+05	0.22818450E+06	0.13970060E+01
79	0.51170000E+04	0.72754536E+01	0.28760973E+05	0.20924906E+06	0.13667994E+01
80	0.41190000E+04	0.75060520E+01	0.24523777E+05	0.18407669E+06	0.13355961E+01
81	0.34880000E+04	0.77364216E+01	0.20048102E+05	0.15510056E+06	0.13053665E+01
82	0.30640000E+04	0.79810381E+01	0.23378184E+05	0.18658212E+06	0.12742376E+01
83	0.25400000E+04	0.82399931E+01	0.26321340E+05	0.21688762E+06	0.12423067E+01
84	0.56600000E+03	0.84989939E+01	0.23177043E+05	0.19698150E+06	0.12113581E+01
85	0.30000000E+01	0.87725449E+01	0.16371875E+05	0.14362300E+06	0.11796789E+01
86	0.0	0.90607738E+01	0.33593647E+04	0.30438441E+05	0.11473513E+01
87	0.0	0.93638382E+01	0.15811874E+02	0.14805983E+03	0.11144505E+01
88	0.0	0.96815305E+01	0.0	0.0	0.10810442E+01
89	0.0	0.10000733E+02	0.0	0.0	0.10486469E+01
90	0.0	0.10334915E+02	0.0	0.0	0.10157776E+01
91	0.20000000E+01	0.10684689E+02	0.0	0.0	0.98249459E+00
92	0.20000000E+01	0.11050324E+02	0.0	0.0	0.94884640E+00
93	0.30000000E+01	0.11432078E+02	0.10268318E+02	0.11738821E+03	0.91488296E+00
94	0.10000000E+01	0.11830269E+02	0.14623405E+02	0.17299879E+03	0.88064480E+00
95	0.0	0.12245192E+02	0.16048706E+02	0.19651947E+03	0.84617281E+00
96	0.0	0.12677209E+02	0.45428343E+01	0.57590454E+02	0.81150061E+00
97	0.0	0.13141702E+02	0.0	0.0	0.77551579E+00
98	0.0	0.13624195E+02	0.0	0.0	0.73945904E+00

ENERGY SPECTRUM FROM A PULSE-HEIGHT DISTRIBUTION

CALIFORNIUM NEUTRON SPECTRUM MEASURED WITH A NE-213 DETECTOR

RUN 13. 8.72. 2 Y-CHANNEL = 1

CONDENSATION IN FEW ENERGY GROUPS

GROUP	UPPER ENERGY (MEV)	UNITARY FLUX(E)	INTEGRATED FLUX	UNITARY FLUX(U)	UPPER LETHARGY
1	14.1000	0.0	0.0	0.0	0.70513147E+00
2	14.0000	0.0	0.0	0.0	0.71224880E+00
3	10.5000	0.70383516E+04	0.15836293E+05	0.65493672E+05	0.99993092E+00
4	8.2500	0.31707008E+05	0.55487270E+05	0.23249056E+06	0.12410927E+01
5	6.5000	0.86114937E+05	0.11969981E+06	0.49675250E+06	0.14795036E+01
6	5.1100	0.19226512E+06	0.21341425E+06	0.86995356E+06	0.17201071E+01
7	4.0000	0.35359331E+06	0.29701844E+06	0.12571900E+07	0.19650116E+01
8	3.1600	0.58986569E+06	0.38932450E+06	0.16559990E+07	0.22007341E+01
9	2.5000	0.88912494E+06	0.56014881E+06	0.19208130E+07	0.24350157E+01
10	1.8700	0.10011721E+07	0.47055119E+06	0.16138720E+07	0.27253675E+01
11	1.4000	0.0	0.0	0.0	0.30148344E+01
12	1.0580	0.0	0.0	0.0	0.32949257E+01
13	0.8000	0.0	0.0	0.0	0.35744495E+01
14	0.5650	0.0	0.0	0.0	0.39222355E+01
15	0.4000	0.0	0.0	0.0	0.42675972E+01
16	0.2828	0.0	0.0	0.0	0.46143217E+01

Table B (Continuation)

Table B (Continuation)

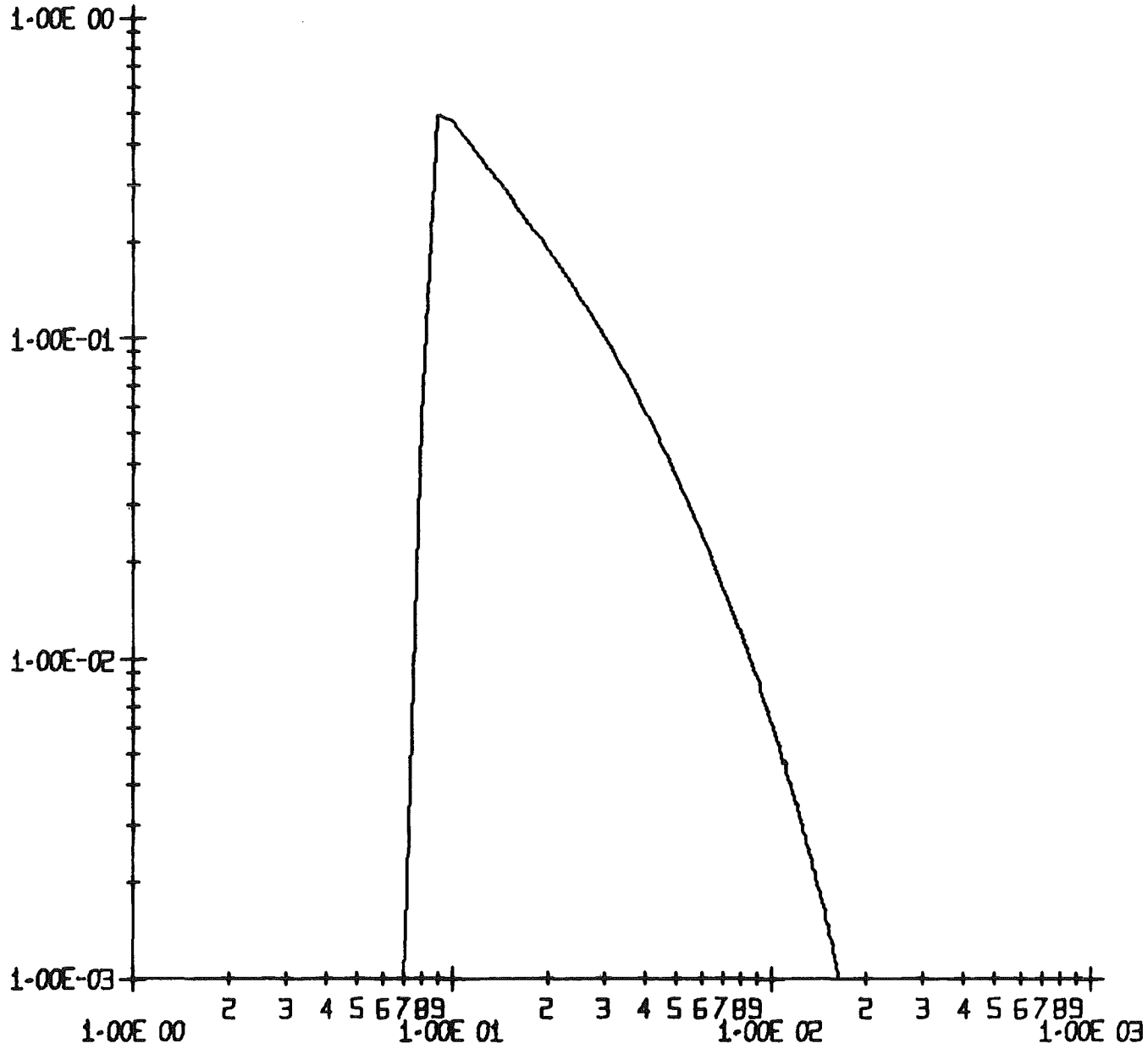

Table B (Continuation)

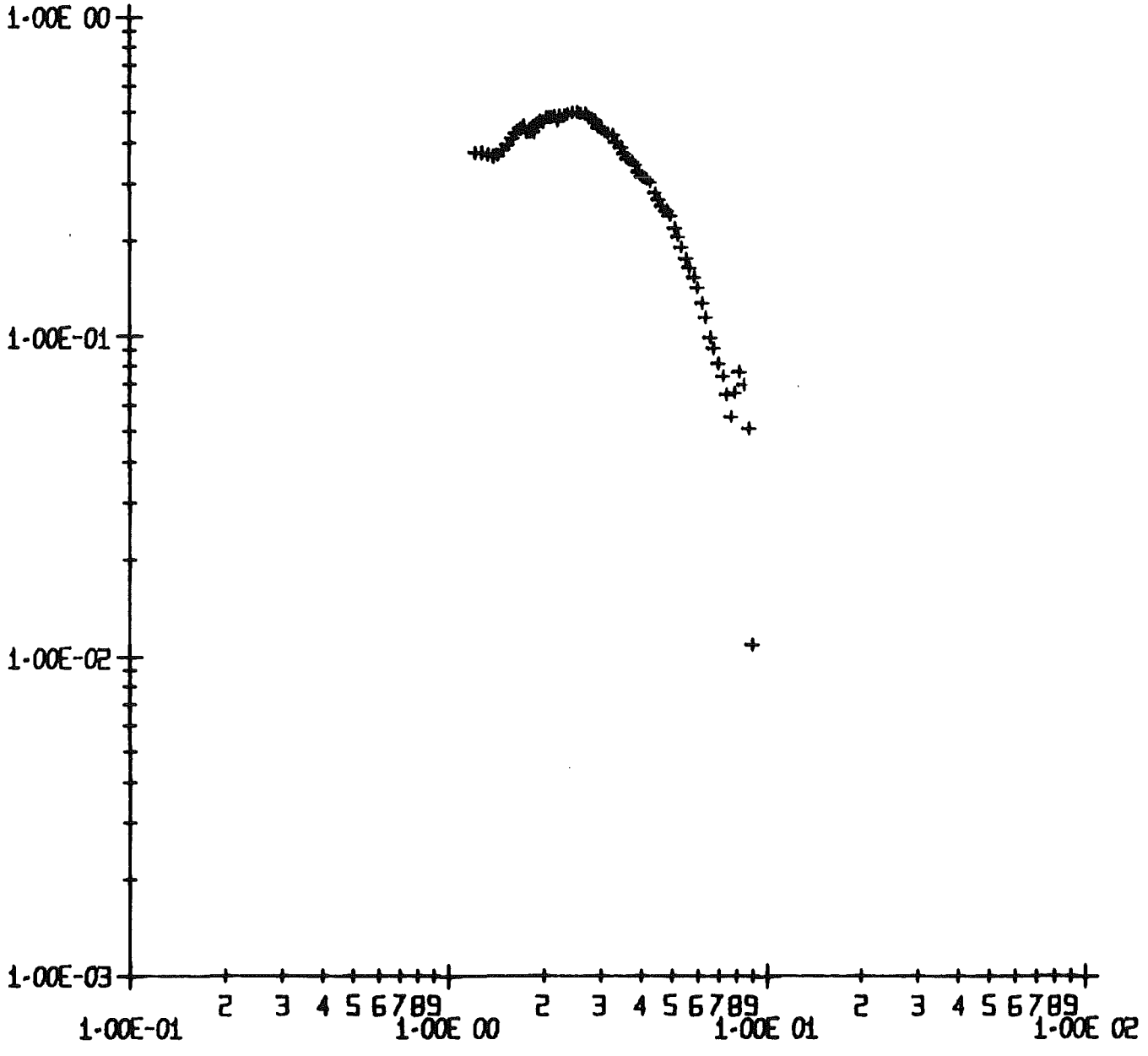

ABB-00001 CALIFORNIUM MEASUREMENT - UNITARY FLUX(U) VS- ENERGY(MEV)

Table B (Continuation)

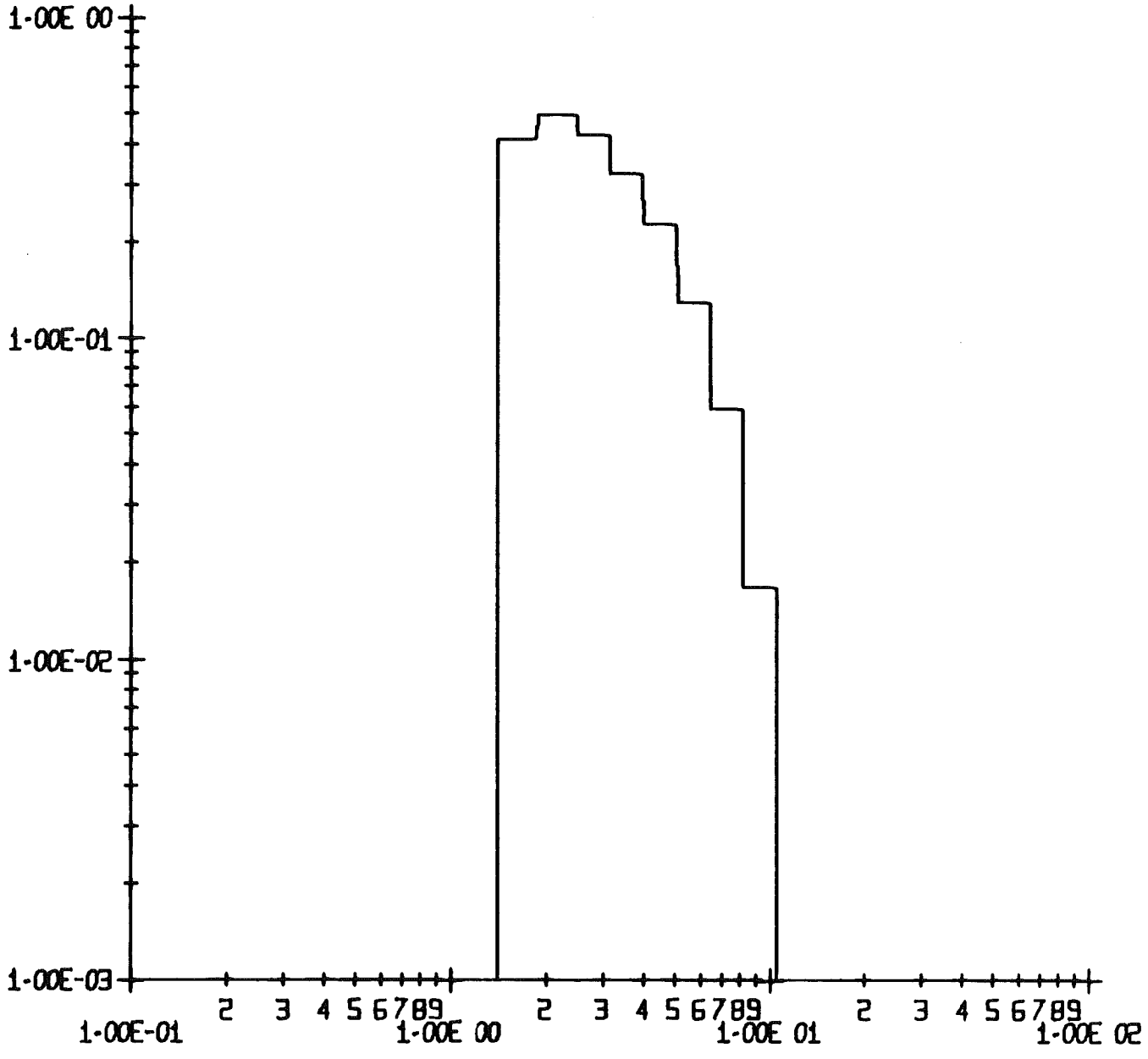

ABB-00001 CALIFORNIUM MEASUREMENT - GROUP FLUX(U) VS- ENERGY(MEV)

Appendix B TRADI Fortran source listing

```
                    MAIN

   ENERGY SPECTRUM FROM A PULSE-HEIGHT DISTRIBUTION

   DIMENSION R(520),RE(520),R1(520),T(520),TS(520),E(520),E1(520),
  XE2(520),U(520),FU(520),AI(6),EC(30),FC(30),EP(60),FP(60),FI(30),
  XIDENT(15),IDCN(15),IDUF(15),IDGF(15),UC(30),FUC(30)

   READ (5,31) AH,AC,DIR,DIL
   READ (5,34) KM,EU
   READ(5,35) (EC(K),K=1,KM)
   READ (5,25) (AI(I),I=1,6)
11 READ (5,1) KD,M,KYE,NM,NU,LI,LY
   IF (KD.EQ.C) STOP
   L=1
   IL=1
   READ (5,3C) ES,IANF,IFIT
   READ (5,2) RESU,CF
   READ (5,10) LCN,LUF,LGF
   READ (5,12) IDENT
   IF (LCN.EC.1) READ (5,12) IDCN
   IF (LUF.EC.1) READ (5,12) IDUF
   IF (LGF.EC.1) READ (5,12) IDGF
   WRITE (6,28) IDENT,KD,M,KYE,NM,L
   WRITE (6,32) ES,IANF,IFIT,RESU
   WRITE(6,26) CF,(AI(I),I=1,6)
   WRITE (6,33) AH,AC,DIR,DIL

 4 READ (NU) IENDE,(T(I),I=1,IENDE)
   IL=IL+1
   IF (IL.LE.LI) GC TC 4
   WRITE (6,28) IDENT,KD,M,KYE,NM,L
   WRITE (6,3)
   WRITE (6,13) (I,T(I), I=1,IENDE)
   IF (LCN.EQ.0) GC TC 7

   PLOTTING  CF  COUNT NUMBER

   DO 87 I=1,IENDE
   TS(I)=T(I)
   E(I)=I
87 CONTINUE
   CALL NORMA (1,IENDE,1.,0.001,1.,E,TS)
   CALL PLOTA(E,TS,IENDE,2,3,1,1,1,-2,3.,0.,C.005080,0.,-3,,0.C05080,
  XIDCN,
  XL,-1,1.,0,1000.,4HE9.2,1,-1,1,1,-1,0.001,0,1.,4HE9.2,1,1,-1,2)
 7 CONTINUE

   CALL CONVER (IENDE,CF,AI,Y,Y1,Y2)

   CALL RESOLL(IANF,IENCE,RESC,T,E,E1,E2,Y,Y1,Y2,R,RE)

   IENDE=IENCE-IFIT
   CALL ABLEIT(IANF,IENDE,IFIT,E,RE,R1)

   CALL FLUX (DIR,DIL,AH,AC,ES,EU,IANF,IENDE,E,R1,U,FU)

   WRITE (6,28) IDENT,KD,M,KYE,NM,L
   WRITE(6,29) EU
```

```
      WRITE (6,6) (I,R(I),E(I),R1(I),FU(I),U(I),I=IANF,IENDE)
      WRITE (6,28) ICENT,KC,M,KYE,NM,L
      CALL FLUXCC (R1,E1,E2,KM,IANF,IENDE,EC,EU,FU,FC,FUC,FI)

      IF (LUF.EQ.0) GO TO 8
      IE=IENDE
      CALL NORMA (IANF,IE,C.1,0.001,1.,E,FU)
      CALL PLOTA(E,FU,IE,1,3,1,2,1,-2,2.,-1.,0.005080,0.,-3.,0.005080,
     XIDUF,
     XL,-1,0.1,0,100.,4HE9.2,1,-1,1,1,-1,0.001,0,1.,4HE9.2,1,1,-1,2)
    8 CONTINUE

      IF (LGF.EQ.0) GO TO 9
      CALL STEPLC (KM,EC,FUC,EP,FP)
      K2=2*KM
      CALL NORMA (1,K2,C.1,C.001,1.,EP,FP)
      CALL PLOTA(EP,FP,K2,2,3,1,1,1,-2,2.,-1.,0.005080,0.,-3.,0.005080,
     XIDGF,
     XL,-1,C.1,C,1CC.,4HE9.2,1,-1,1,1,-1,0.001,0,1.,4HE9.2,1,1,-1,2)
    9 CONTINUE
      L=L+1
      IF (L.LE.LY) GO TO 4
      REWIND NU
      GO TO 11

   31 FORMAT (2F7.6,2F4.2)
   34 FORMAT (I3,F6.3)
   35 FORMAT (1CF7.4)
   25 FORMAT (6F10.8)
    1 FORMAT (6I2,I4)
   30 FORMAT (F4.3,2I4)
    2 FORMAT (F3.3,F6.3)
   10 FORMAT (3I2)
   12 FORMAT (15A4)
    3 FORMAT (/3CX,' EXPERIMENTAL  PULSE-HEIGHT  DISTRIBUTION'//)
   13 FORMAT (9(I5,F8.0))
   28 FORMAT (1H1,25X,'   ENERGY SPECTRUM FROM A PULSE-HEIGHT DISTRIBUTI
     XON',//,25X,15A4,
     1//30X,'RUN',I5,'.',I2,'.',I2,'.',I2,5X,'Y-CHANNEL = ',I2//)
   32 FORMAT (10X,'THRESHOLD ENERGY =',F6.3,' MEV'//10X,'INITIAL CHANNEL
     X IANF =',I3//1CX,'GROUPED CHANNELS IFIT =',I3//10X,
     X'PULSE HEIGHT RESOLUTION =',F6.3////)
   26 FORMAT (10X,'CALIBRATION FACTOR CF =',F8.3//10X,'TRANSFORMATION CO
     XEFFICIENTS :'//20X,'A(1) =',F12.8/20X,'A(2) =',F12.8/20X,'A(3) =',
     XF12.8/20X,'A(4) =',F12.8/20X,'A(5) =',F12.8/20X,'A(6) =',F12.8///)
   33 FORMAT(10X,'H-ATOMS = ',F8.6,'E 24  1/CM3'/10X,'C-ATOMS = ',F8.6,
     X'E 24  1/CM3'//10X,'DETECTOR-RADIUS = ',F4.2,' CM'/10X,'DETECTOR-L
     XENGHT = ',F4.2,' CM')
   29 FORMAT (' CHANNEL',10X,'COUNT NUMBER',10X,'MEAN ENERGY',10X,
     X'UNITARY FLUX',10X,'UNITARY FLUX',10X,'MEAN LETHARGY'/
     X' (COMB.)',11X,'(COMBINED)',14X,'(MEV)',15X,
     X'(ENERGY)',13X,'(LETHARGY)',9X,'(U=0 FOR ',F5.2,' MEV)'//)
    6 FORMAT (I5,6X,E20.8,1X,E20.8,2X,E20.8,2X,E20.8,3X,E20.8)
      END
```

CONVER

```
      SUBROUTINE CONVER (IENDE,CF,AI,Y,Y1,Y2)

      CONVERTION:  LOG(E) = SUM (A(I)*(LOG(V))**(I-1)),    I=1,6

      DIMENSION AI(6)
      REAL*8 SI1,SI2,S1,S2,SI,S,Y(520),Y1(520),Y2(520)
      Y(1)=0.
      DO 21 IE=2,IENDE
      SA=IE
      SI=(SA-1.)*CF
      SI1=(SA-1.5)*CF
      SI2=(SA-0.5)*CF
      S=0.
      S1=0.
      S2=0.
      DO 22 I=1,6
      S=S+AI(I)*(DLOG10(SI))**(I-1)
      S1=S1+AI(I)*(DLOG10(SI1))**(I-1)
      S2=S2+AI(I)*(DLOG10(SI2))**(I-1)
   22 CONTINUE
      S=S*2.302585
      S1=S1*2.302585
      S2=S2*2.302585
      Y(IE)=DEXP(S)
      Y1(IE)=DEXP(S1)
      Y2(IE)=DEXP(S2)
   21 CONTINUE
      RETURN
      END
```

RESOLU

```
      SUBROUTINE RESCLU(IANF,IENDE,RESU,T,E,E1,E2,Y,Y1,Y2,R,RE)

            ***  RESCLUTION  CORRECTION  ***

      DIMENSION T(520),R(52C),E(520),E1(520),E2(520),RE(520)
      REAL*8 Y(520),Y1(520),Y2(520),DELTA(520)
      IQ=IANF-1
      DO 3 I=1,IC
      E(I)=Y(I)
    3 CONTINUE
      IC=IANF
      I=IANF
  702 TA=I*RESU
      KA=TA
      DA=TA-KA
      IF (DA.GE.C.5) KA=KA+1
      IF(KA.EQ.0) KA=1
      IF ((I+KA).GT.IENDE) KA=IENDE-I
      W=0.
      Z=0.
      IKA=I+KA-1
      DO 701 JL=1,IKA
      W=W+T(JL)
  701 CONTINUE
      DO 1 NN=I,IKA
      Z=Z+Y(NN)
    1 CONTINUE
      R(IC)=W
      E(IC)=Z/KA
      E1(IC)=Y1(I)
      E2(IC)=Y2(IKA)
      I=IKA+1
      IF (I.GE.IENDE) GO TO 703
      IC=IC+1
      GO TO 702
  703 IENDE=IC
      E1(IENDE+1)=E2(IENDE)
      DO 13 I=IANF,IENDE
      DELTA(I)=E1(I+1)-E1(I)
      RE(I)=R(I)/(DELTA(I))
   13 CONTINUE
      RETURN
      END
```

ABLEIT

```
      SUBROUTINE ABLEIT(IANF,IENDE,IFIT,ABSZ,EIN,AUS)

      SECOND  ORDER  POLYNOMIAL  FITTING  AND  DIFFERENTIATION
                     OF A PULSE-HEIGHT  DISTRIBUTION

      DIMENSION ABSZ(520),EIN(520),AUS(520)
      REAL*8 U(3,3),V(3),S(3)
      I1=(IFIT-1)/2
      II=IANF+I1
      IJ=IENDE-I1
      DO 2 I=II,IJ
      J=I-I1-1
      DO 3 L=1,3
      V(L)=0.
      DO 3 K=1,3
    3 U(K,L)=0.
      DO 4 M=1,IFIT
      JM=J+M
      X1=ABSZ(JM)-ABSZ(I)
      X2=X1**2
      X3=X2*X1
      X4=X2*X2
      V(1)=V(1)+EIN(JM)*X2
      V(2)=V(2)+EIN(JM)*X1
      V(3)=V(3)+EIN(JM)
      U(1,1)=U(1,1)+X4
      U(1,2)=U(1,2)+X3
      U(1,3)=U(1,3)+X2
      U(2,1)=U(1,2)
      U(2,2)=U(1,3)
      U(2,3)=U(2,3)+X1
      U(3,1)=U(1,3)
      U(3,2)=U(2,3)
    4 U(3,3)=U(3,3)+1
      CALL GAUSS3(3,U,V,S,IC)
      IF(IC) 12,13,12
   12 WRITE(6,60)
   60 FORMAT(' MATRIX U SINGULAER')
      S(2)=0
      GOTO 2
   13 CONTINUE
      IF(I.EQ.II)GOTO5
      IF(I-IJ)2,6,2
    5 DO 7 N=IANF,II
      X1=ABSZ(N)-ABSZ(II)
    7 AUS(N)=2*S(1)*X1+S(2)
      GOTO 2
    6 DO 8 N=IJ,IENDE
      X1=ABSZ(N)-ABSZ(IJ)
    8 AUS(N)=2*S(1)*X1+S(2)
    2 AUS(I)=S(2)
      IK=IANF-1
      DO 9 I=1,IK
    9 AUS(I)=0.
      RETURN
      END
```

SIGMA

```
FUNCTION SIGMA(E)

CALCULATION OF THE N-P CROSS SECTION

H1=0.09415*E-1.86+C.0CC13*E**2
H1=3/(1.206*E+1**2)
H2=(0.4223+0.13*E)**2+1.206*E
SIGMA=3.141593*(H1+1/H2)
RETURN
END
```

FLUX

```
      SUBROUTINE FLUX (DIR,DIL,AH,AC,ES,EU,IANF,IENDE,E,R1,U,FU)

      FLUX PER UNIT ENERGY AND LETHARGY

      DIMENSION E(520),R1(520),U(520),FU(520)
      S=3.141593*DIR**2.
      DO 2 I=IANF,IENDE
      EN=E(I)
      SH=SIGMA(EN)
      SC=2.285*EN**(-0.425)
      A=AH*SH+AC*SC
      AL=A*DIL
      F=(1-EXP(-AL))/AL

      EFFICIENCY CORRECTION
      EPSI=AH*SH*DIL*F

      DOUBLE SCATTERING AND WALL EFFECT CORRECTION

      C1=0.78/DIL
      C2=0.09*DIL*AH
      C3=0.077*DIR*AH
      RMAX=1.18*10**(-3)*EN**1.75
      SIG1=SIGMA(0.068*EN)
      ETA=1-C1*RMAX+C2*SH+C3*SIG1
      R1(I)=-(EN*R1(I))/(S*EPSI*ETA)
      IF (EN.LE.ES) R1(I)=0.
    2 CONTINUE

      DO 43 I=IANF,IENDE
      IF (R1(I).LT.0.) R1(I)=0.
      FU(I)=E(I)*R1(I)
      AR=EU/E(I)
      U(I)=ALOG(AR)
   43 CONTINUE
      RETURN
      END
```

FLUXCO

```
      SUBROUTINE FLUXCO (R,E1,E2,M,IA,IE,EC,EU,FU,FC,FUC,FI)

      FLUX CONDENSATION IN FEW ENERGY GROUPS

      DIMENSION R(520),EC(30),FC(30),FI(30),
     XE1(520),E2(520),IK(30),UC(30),FUC(30),FU(520)
      DO 12 K=1,M
      AR=EU/EC(K)
      UC(K)=ALOG(AR)
   12 CONTINUE
      EMAX=E2(IE)
      K=1
   11 IF (EMAX-EC(K)) 9,10,10
    9 FC(K)=0.
      FI(K)=0.
      FUC(K)=0.
      K=K+1
      GO TO 11
   10 KI=K
      EC(M+1)=0.
      K=M
      S=0.
      SU=0.
      I=IA
      EMIN=E1(IA)
   19 IF (EC(K)-EMIN) 17,18,20
   17 FC(K)=0.
      FI(K)=0.
      FUC(K)=0.
      K=K-1
      GO TO 19
   18 FC(K)=0.
      FI(K)=0.
      FUC(K)=0.
      K=K-1
      GO TO 4
   20 FC(K)=0.
      FI(K)=0.
      FUC(K)=0.
   24 IF (E1(I)-EC(K)) 21,22,23
   21 I=I+1
      GO TO 24
   22 K=K-1
      GO TO 4
   23 S=R(I-1)*(E1(I)-EC(K))
      AR1=EU/E1(I)
      U1=ALOG(AR1)
      SU=FU(I-1)*(UC(K)-U1)
      K=K-1
    4 IF (E2(I)-EC(K)) 1,2,3
    1 S=S+R(I)*(E2(I)-E1(I))
      AR1=EU/E1(I)
      AR2=EU/E2(I)
      U1=ALOG(AR1)
      U2=ALOG(AR2)
      SU=SU+FU(I)*(U1-U2)
      I=I+1
      GO TO 4
```

FLLXCC

```
 2 S=S+R(I)*(E2(I)-E1(I))
   FC(K)=S/(EC(K)-EC(K+1))
   FI(K)=S
   IF (K.EQ.M) GO TO 13
   AR1=EU/E1(I)
   AR2=EU/E2(I)
   U1=ALOG(AR1)
   U2=ALOG(AR2)
   SU=SU+FU(I)*(U1-U2)
   FUC(K)=SU/(UC(K+1)-UC(K))
   GO TO 15
13 FUC(K)=FC(K)*EC(M)/2.
15 S=0.
   SU=0.
   I=I+1
   K=K-1
   IF (K-KI) 5,4,4
 3 S=S+R(I)*(EC(K)-E1(I))
   FC(K)=S/(EC(K)-EC(K+1))
   FI(K)=S
   IF (K.EQ.M) GO TO 14
   AR1=EU/E1(I)
   U1=ALOG(AR1)
   SU=SU+FU(I)*(U1-UC(K))
   FUC(K)=SU/(UC(K+1)-UC(K))
   GO TO 16
14 FUC(K)= FC(K)*EC(M)/2.
16 AR2=EU/E2(I)
   U2=ALOG(AR2)
   SU=FU(I)*(UC(K)-U2)
   S=R(I)*(E2(I)-EC(K))
   K=K-1
   IF (E2(I).LT.EC(K)) GO TO 25
   S=S-R(I)*(E2(I)-EC(K))
   FC(K)=S/(EC(K)-EC(K+1))
   FI(K)=S
   SU=SU-FU(I)*(UC(K)-U2)
   FUC(K)=SU/(UC(K+1)-UC(K))
   S=R(I)*(E2(I)-EC(K))
   SU=FU(I)*(UC(K)-U2)
   K=K-1
25 I=I+1
   IF (K-KI) 5,4,4
 5 WRITE (6,6)
 6 FORMAT(37X,'CONDENSATION IN FEW ENERGY GROUPS'//
  X' GROUP',6X,'UPPER ENERGY (MEV)',8X,'UNITARY FLUX(E)',6X,
  X'INTEGRATED FLUX',8X,'UNITARY FLUX(U)',7X,'UPPER LETHARGY'//)
   K=1
   DO 8 I=1,M
   IK(K)=I
   K=K+1
 8 CONTINUE
   WRITE(6,7) (IK(K),EC(K),FC(K),FI(K),FUC(K),UC(K),K=1,M)
 7 FORMAT (I4,12X,F7.4,9X,E20.8,4X,E18.8,3X,E20.8,3X,E18.8)
   RETURN
   END
```

NORMA

```
      SUBROUTINE NORMA (IANF,IENDE,XA,YA,YE,E,FU)

      NORMALIZATION  TO  THREE  DECADES

      DIMENSION E(520),FU(520)
      IAN=IANF-1
      YFU=FU(IANF)/10.
      DO 8 I=IANF,IENDE
      FR=FU(I)
      YFU=AMAX1(FR,YFU)
    8 CONTINUE
      COEF=0.5*YE/YFU
      DO 9 I=IANF,IENDE
      FU(I)=COEF*FU(I)
      IF (FU(I).LE.0.) FU(I)=YA/100.
      FU(I)=ALOG10(FU(I))
      IF (E(I).LE.0.) E(I)=XA/100.
      E(I)=ALOG10(E(I))
    9 CONTINUE
      DO 10 I=1,IAN
      FU(I)=YA/100.
      FU(I)=ALOG10(FU(I))
      IF (E(I).LE.0.) E(I)=XA/100.
      E(I)=ALOG10(E(I))
   10 CONTINUE
      RETURN
      END
```

STEPLO

```
      SUBROUTINE STEPLO (K,E,F,EP,FP)

      STEP  FUNCTION  FOR  PLOTTING

      DIMENSION E(30),F(30),EP(60),FP(60)
      E(K+1)=0.
      DO 1 I=1,K
      EP(2*I-1)=E(I)
      FP(2*I-1)=F(I)
      EP(2*I)= E(I+1)+(E(I)-E(I+1))/100.
      FP(2*I)=F(I)
    1 CONTINUE
      RETURN
      END
```

Appendix C Transfer of measured count number to a magnetic tape for input in TRADI

Usually the count number registered in the memory of a multichannel analyzer is obtained in the form of a punched tape. To transfer this data in a form suitable for input to the TRADI code the procedure shown in Fig. b is applied.

The first step, transfer of the data from the punched tape to a direct access unit (NUSYS Disc) is done by using the code LOLE /41/.

The second step, transfer of the data from the direct access unit to the magnetic tape, is done by using the code PLABA. A listing of this program is given in Appendix D. PLABA records the data on the tape in a form that can be directly used as input in TRADI.

The input cards required for PLABA, in standard FORTRAN convention, are the following:

Card 1 : (I2)

INM = number of measurements to transfer

Card 2 : (5I2,I4)

KD = number corresponding to the day of measurement

KM = number corresponding to the month of measurement

KA = last two numbers corresponding to the year of measurement

ID = number of channels in Y-direction. For a monodimensional measurement ID = 1

IENDE = number of channels in X-direction

If INM>1 add the corresponding Cards "2".

In the unit declaration cards the corresponding LABEL-number and DSN-designation must be given.

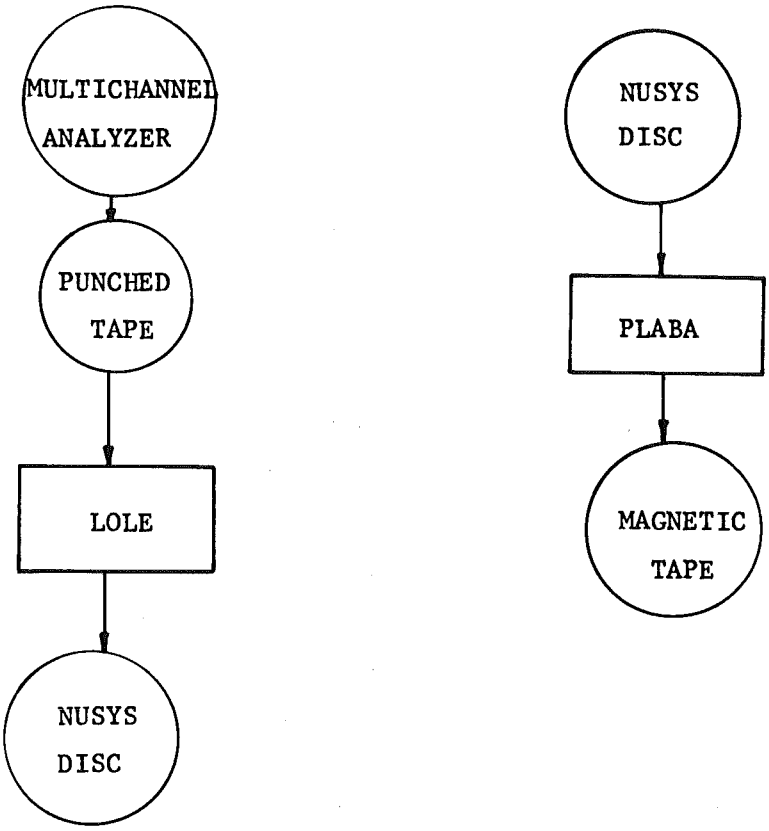

Fig. b: Transferring of data from punched tape to a magnetic tape for use as input in TRADI code

Appendix D Listing of the PLABA code

```
*****************************************************************
*                                                               *
*                          PLABA                                *
*                                                               *
*     MESSDATEN  VON  NUSYS  PLATTE  AUF  BAND  SCHREIBEN      *
*                                                               *
*****************************************************************

      DIMENSION R(4100),KANIN(4100),IK(4100)
      READ(5,5) INM
      LK=0
    7 READ(5,1) KD,KM,KA,NM,ID,IENDE
   13 READ (1) NAME,MESS
      READ(1) K,(KANIN(I),I=1,K)
      DO 10 I=1,K
      R(I)=KANIN(I)
   10 CONTINUE
      LK=LK+1
      WRITE(6,2) KD,KM,KA,NM
      KF=0
      DO 4 KY=1,ID
      KI=KF+1
      KF=KI+IENDE-1
      WRITE(2) IENDE,(R(I),I=KI,KF)
   14 WRITE (6,3) KY,IENDE
      DO 18 I=KI,KF
      IK(I)=I-(KY-1)*IENDE
   18 CONTINUE
      WRITE(6,9) (IK(I),R(I),I=KI,KF)
    4 CONTINUE
      IF (LK.LT.INM) GO TO 7
      END FILE 2
      REWIND 2
    5 FORMAT (I2)
    1 FORMAT (5I2,I4)
    2 FORMAT (//'          MESSUNG NR.  ',I2,'.',I2,'.',I2,'.',I2,//)
    3 FORMAT (//'           Y-KANAL =',I3,'          ANZAHL X-KANAELE =',
     X     I5,/)
    9 FORMAT (9(I5,F8.0))
      STOP
      END
```

REFERENCES

/1/ A. Prince

Analysis of high energy neutron cross sections for fissile and fertile isotopes

Proc. Second Int. Conf. on Nucl. Data for Reactors, Vol. II, IAEA, 1970, p. 825.

/2/ J. Kallfelz, B. Zolotar and B. Sehgal

Modifications to fissile element cross sections and their influence on calculated fast reactor parameters

ANL-7610 (1969) 224.

/3/ E. Kiefhaber and D. Thiem

The influence of fission neutron spectra on integral nuclear quantities of fast reactors

KFK-1561 (1972).

/4/ T. Gozani

Experimental kinetics studies in a ^{238}U sphere

Nucl. Sci. Eng. 36, 143 (1969).

/5/ D. Rusch, N. Pieroni and E. Wattecamps

Berechnung und Messung zeitabhängiger Neutronenspektren einer gepulsten Natururananordnung

KFK-1272/2 (1972) 121-3.

/6/ H. Borgwaldt, M. Küchle, F. Mitzel and E. Wattecamps
SUAK - A fast subcritical facility for pulsed neutron measurements
IAEA-Symp., Karlsruhe, 1965, SM 62/3.

/7/ D. Rusch
Eine gepulste 14 MeV Neutronenquelle mit Klystron-Strahlgruppierung zur Erzeugung kurzer Pulse hoher Intensität
KFK-1271/2 or EUR 472d, 1971.

/8/ H. Küsters (comp.)
Progress in fast reactor physics in the Federal Republic of Germany
KFK-1632 or EACRP-U-46, 1973, Sect. 3.2.3.

/9/ J.J. Schmidt
Neutron cross sections for fast reactor materials
KFK-120 or EANDC-E-35 U, 1966.

/10/ D. Rusch, personal communication.

/11/ N. Pieroni, D. Rusch and E. Wattecamps
Measurement of time-dependent fast neutron spectra with a NE 213 scintillator
Nucl. Instr. and Meth. 115 (1974) 317.

/12/ D. Decke and C. Williams
High resolution time spectrometry
ORTEC, 1968.

/13/ V. Verbinsky, W. Burrus, T. Love, W. Zobel, N. Hill and R. Textor

Calibration of an organic scintillator for neutron spectrometry

Nucl. Instr. and Meth. 65 (1968) 8.

/14/ F. Kappler, D. Rusch and E. Wattecamps

Detection efficiency of fast neutron time-of-flight detectors and reliability check by measuring tailored source spectra

Nucl. Instr. and Meth. 111 (1973) 83.

/15/ D. Smith, R. Polk and T. Miller

Measurement of the response of several organic scintillators to electrons, protons and deuterons

Nucl. Instr. and Meth. 64 (1968) 157.

/16/ A. Wickenhäuser

Beschreibung einiger FORTRAN-Subroutinen allgemeinen Inhalts in der IASR-Programmbibliothek

unpublished.

/17/ J. Marion and J. Fowler (ed.)

Fast Neutron Physics

New York, Interscience Publishers, 1963.

/18/ G. Halbritter

Die Spektrometrie schneller Neutronen mit festen organischen Szintillatoren

Diplomarbeit, Institut für Meß- und Regel. der Technischen Hochschule München, 1969.

/19/ H. Broeck and C. Anderson

The stilbene scintillation crystal as a spectrometer for continuous fast-neutron spectra

Rev. of Sci. Instr. 31, 10 (1960) 1063.

/20/ M. Toms

Stilbene and NE 213 characteristics related to their use for neutron spectrometry

IEEE Trans. Nucl. Sci. NS-17, No. 3 (1970) 107.

/21/ W. Burrus and V. Verbinski

Fast-neutron spectroscopy with thick organic scintillators

Nucl. Instr. and Meth. 67 (1969) 181.

/22/ H. Werle and H. Bluhm

Fission-neutron spectra measurements of ^{235}U, ^{239}Pu and ^{252}Cf

Jour. of Nucl. Energ. 26 (1972) 165.

/23/ E. Barnard, C. Ferguson, W. McMurray and I. van Heerden

Time-of-flight measurements of neutron spectra from the fission of ^{235}U, ^{238}U and ^{239}Pu

Nucl. Phys. 71 (1965) 228.

/24/ H.H. Knitter, A. Paulsen, H. Liskien and M.M. Islam

Measurements of the neutron energy spectrum of the spontaneous fission of ^{252}Cf

Atomkernenergie (ATKE) 22 (1973) 1fg. 2., 84.

/25/ E. Straker, C. Burgart, T. Love and R. Freestone

Simultaneous determination of fast-neutron spectra by time-of-flight and pulse-height unfolding techniques

Nucl. Instr. and Meth. 97 (1971) 275.

/26/ W. Eyrich
Zwei leistungsstarke Neutronengeneratoren für Impuls- und Dauerbetrieb
Nukleonik 4, 4 (1962) 167.

/27/ G. Arnecke, H. Borgwaldt and M. Lalovic
Kurzbeschreibung des Karlsruher Monte-Carlo Codes KAMCCO
unpublished.

/28/ G. Arnecke, H. Borgwaldt and M. Lalovic
DASU-Programm zur Erstellung von Wirkungsquerschnitten für den Monte-Carlo Code KAMCCO
unpublished.

/29/ H. Borgwaldt
DACONT-Programmbeschreibung (in preparation).

/30/ H. Borgwaldt, personal communication.

/31/ J.J. Schmidt
Fast neutron nuclear data for ^{238}U
KFK-120/Teil I, Abschnitt VI-2 (1966).

/32/ N. Pieroni, E. Wattecamps and D. Rusch
Preliminary results of a new method for investigating fast neutron cross section data
unpublished.

/33/ H. Bluhm

Neutronenspektrumsmessungen in einem abgereicherten Uranmetallblock zur Untersuchung von diskrepanten ^{238}U-Wirkungsquerschnitten

KFK-1798 (1973).

/34/ D. Rusch, N. Pieroni and E. Wattecamps

Ein-Material-Experimente an der SUAK: Ausflußspektrum der Anordnung UNAT, experimentelles Ergebnis und erste Rechnungen

unpublished.

/35/ J. Chaudat, M. Darrouzet and E. Fischer

Experiments in pure uranium lattices with unit k_∞. Assemblies SNEAK-8/8Z; UK 1 and UK 5 in ERMINE and HARMONIE

KFK-1865 or CEA-R-4552, 1974.

/36/ P. McGrath

KAPER - Lattice program for heterogeneous critical facilities (User's guide)

KFK-1893 (1973).

/37/ E. Kiefhaber (comp.)

The KFKINR-set of group constants; nuclear data basis and first results of its application to the recalculation of fast zero-power reactors

KFK-1572 (1972).

/38/ E. Kiefhaber, personal communication.

/39/ G. Halbritter, personal communication.

/40/ S. Heine
PLOTA, ein verallgemeinertes Plot-Programm
unpublished.

/41/ M. Ferranti and F. Kappler
Programme zur Auswertung von Neutronenspektrumsmessungen nach der Flugzeitmethode
unpublished.